J. Phycol. **42,** 434–452 (2006)

DOI: 10.1111/j.1529-8817.2006.00195.x

ULTRASTRUCTURE AND LSU rDNA-BASED PHYLOGENY OF *ESOPTRODINIUM GEMMA* (DINOPHYCEAE), WITH NOTES ON FEEDING BEHAVIOR AND THE DESCRIPTION OF THE FLAGELLAR BASE AREA OF A PLANOZYGOTE[1]

António J. Calado,[2] *Sandra C. Craveiro*

Departamento de Biologia, Universidade de Aveiro, P-3810-193 Aveiro, Portugal

Niels Daugbjerg and Øjvind Moestrup

Department of Phycology, Biological Institute, University of Copenhagen, Øster Farimagsgade 2D, DK-1353 Copenhagen K, Denmark

A small, freshwater dinoflagellate with an incomplete cingulum, identified as *Esoptrodinium gemma* Javornický (=*Bernardinium bernardinense* sensu auctt. non sensu Chodat), was maintained in mixed culture and examined using light and serial section TEM. Vegetative flagellate cells, large cells with two longitudinal flagella (planozygotes), and cysts were examined. The cells displayed a red eyespot near the base of the longitudinal flagellum, made of two or three layers of pigment globules not bounded by a membrane. Yellow-green, band-shaped chloroplasts, bounded by three membranes and containing lamella with three thylakoids, were present in both flagellate cells and cysts. Most cells had food vacuoles, containing phagotrophically ingested chlamydomonads or chlorelloid green algae; ingestion occurred through the ventral area, involving a thin pseudopod apparently driven by the peduncle. The pusule was tubular, with numerous diverticula in its distal portion, and opened into the longitudinal flagellar canal. Three roots were associated with each pair of flagellar bases, both in vegetative cells and in a planozygote. The longitudinal microtubular root bifurcated around the longitudinal basal body. The planozygote contained a single peduncle and associated structures, and a single transverse flagellar canal with the two converging transverse flagella. Using two ciliates as outgroup species, phylogenetic analyses based on maximum parsimony, neighbor-joining and posterior probability (Bayesian analysis) supported a clade comprising *Esoptrodinium*, *Tovellia*, and *Jadwigia*.

Key index words: ***Bernardinium bernardinense*; Dinophyceae; *Esoptrodinium gemma*; eyespot; flagellar apparatus; LSU rDNA; phagotrophy; phylogeny; planozygote; ultrastructure**

Abbreviations: **BA, Bayesian analysis; BB, basal body; LB, longitudinal basal body; LMR, longitudinal microtubular root; MCMC, Monte Carlo Markov chains; MP, maximum parsimony; NJ, neighbor-joining; PP, posterior probabilities; PSC, peduncular striated collar; SRC, striated root connective (TSR to LMR); TB, transverse basal body; TMR, transverse microtubular root; TMRE, TMR extension; TSR, transverse striated root; TSRM, transverse striated root microtubule; VR, ventral ridge**

The organism used in this study is a naked dinoflagellate that would be readily identified as *Bernardinium bernardinense* Chodat by recent dinoflagellate floras (Starmach 1974, Matvienko and Litvinenko 1977, Popovský and Pfiester 1990). In his original description of *B. bernardinense*, Chodat (1924, pp. 40–41) mentioned the incomplete cingulum, which disappeared on the dorsal side, and the absence of chloroplasts and of a distinct sulcus. The new genus *Bernardinium* was compared with *Hemidinium* F. Stein, from which it was distinguished mainly by the well-defined sulcus in the two *Hemidinium* species previously described. Although *Hemidinium* was originally described as unarmored (Stein 1878, pp. 91 and 97, 1883, pl. 2, Figs. 23–26), the type species is currently regarded as a thecate form with thin plates (Popovský and Pfiester 1990). The smaller of the two cell portions delimited by the incomplete cingulum was placed on top in Chodat's (1924) original drawings; his description shows he regarded this as the epicone ("parte dimidia superiore"). Schiller (1935) reinterpreted the orientation of the cell and reproduced Chodat's drawings with the longitudinal flagellum emerging downward, pointing out that, with this orientation, the cingulum is directed toward the right side of the body. Huber-Pestalozzi (1950, p. 164) regarded the species as imperfectly described and transferred it to *Hemidinium*.

The second report of an organism identified as *B. bernardinense* is that of Thompson (1951); the cells described resembled Chodat's (1924) in both size and general morphology, but displayed the orientation of cingulum and transverse flagellum that is common in

[1]Received 31 August 2005. Accepted 22 December 2005.
[2]Author for correspondence: e-mail acalado@bio.ua.pt.

dinoflagellates, i.e. to the cell's left. A third and more detailed description of an organism under this name comes from Javornický (1962), whose specimens show the same orientation as those of Thompson (1951). Javornický (1962) considered the orientation shown in Chodat's (1924) drawings to be an error, and Conrad's (1939) comment that *Bernardinium* is an inverse *Hemidinium* to be therefore unjustified. Wawrik (1983) reported the species, with the name *H. bernardinense*, from a pond in Lower Austria (Wawrik 1983, Fig. 1g); a single cell is depicted with the cingulum extending to the viewer's left, although the orientation of the cell was not mentioned and a transverse flagellum was not seen. Popovský (1990) reported *B. bernardinense* with a left hand orientation of the cingulum from ponds in Czechoslovakia, although his drawings show cells with a different general morphology and a well-marked sulcus, making the identification somewhat doubtful.

Javornický (1997) reported a flagellate with the general features ascribed to *B. bernardinense* from a little freshwater pond in Rügen Island, North-East Germany and both the cingulum and the transverse flagellum oriented toward the cell's right; upon comparison with Chodat's (1924) drawings, Javornický (1997) concluded that this German population represented *B. bernardinense* in the original sense of Chodat. Considering the nearly mirror-symmetrical populations studied by both Thompson (1951) and Javornický (1962) to represent not only a different species, but a different genus, Javornický (1997) described the new genus *Esoptrodinium*, with the type species *Esoptrodinium gemma* based on the population described by Javornický (1962) under the name *B. bernardinense*. The organism studied herein has a left-oriented cingulum and transverse flagellum and is therefore identifiable as *E. gemma* Javornický.

The organization of the flagellar base area has been studied in detail for over 20 species of dinoflagellates (Calado and Moestrup 2002, Hansen and Daugbjerg 2004). Although swimming dinoflagellate cells resulting from the fusion of gametes are known to have two longitudinal flagella and the parallel arrangement of the two sets of basal bodies and roots has been shown (Wedemayer and Wilcox 1984), a detailed description of the flagellar base area of a planozygote, such as is given herein for *Esoptrodinium*, has not previously been published. Additionally, we report on the phylogeny of *Esoptrodinium* based on three-cell PCR determination of nuclear-encoded large subunit (LSU) rDNA.

MATERIALS AND METHODS

E. gemma was collected from the sediment of a sidewalk covered by a few centimeters of flowing tap water leaking from a damaged pipe, in the campus of the University of Aveiro, Portugal. Samples were taken repeatedly between June and September 2002 and mixed cultures were prepared in Chu no. 10 medium (Nichols 1973) and kept at 20° C with a 12:12 Light:Dark photoperiod. Some cultures were initiated from the sediment of samples that had dried out, by adding culture medium and exposing it to the light.

Light microscopy. The morphology and swimming mode of cells were recorded with a Sony Video Cassette Recorder SLV-825 (Sony Corporation, Tokyo, Japan). Micrographs were taken with a Leica DMLB light microscope (Leica Microsystems, Wetzlar, Germany) with differential interference contrast. Observations of the feeding process were made in microchambers prepared by attaching a rectangular Plasticine support onto a 24 mm × 32 mm coverslip, placing a drop of the culture in the middle of the coverslip, inverting it over a slide, and pressing along the edges.

Electron microscopy. Cultured material was fixed in a mixture of 1% glutaraldehyde and 0.25% osmium tetroxide (final concentrations) in 0.1 M phosphate buffer, pH 7.2, for 15 min at room temperature. After centrifugation, the pellet was rinsed in the same buffer, embedded in 1.5% agar, and postfixed for approximately 1 h in 1% buffered osmium tetroxide at room temperature. Rinsing in buffer and water, and dehydration through a graded ethanol series up to 70%, was performed at 4° C. After the final dehydration steps in ethanol and propylene oxide, at room temperature, the material was embedded in Epon. Single cells of *E. gemma*, which were greatly outnumbered by green flagellates and other prey organisms, were singled out in the blocks with the light microscope and sectioned with a diamond knife on a Reichert Ultracut E (Leica Microsystems, Wetzlar, Germany). The sections were picked up with slot grids, placed on Formvar film, contrasted with uranyl acetate and lead citrate, and examined with a JEOL JEM 1010 electron microscope (JEOL Ltd., Tokyo, Japan). Serial sections from two vegetative cells, a planozygote and a cyst were examined.

PCR amplification. Using a capillary pipette three cells of *E. gemma* from a culture grown on a species of *Chlamydomonas* were transferred through three rinses in double-distilled water and placed in the same 0.5 mL PCR tube containing 8 µL of double-distilled water. Amplification of partial LSU rDNA using the forward primer "D1F" (Scholin et al. 1994) and the reverse dinoflagellate specific primer "Dino-ND" (Hansen and Daugbjerg 2004) resulted in a PCR product of approximately 1800 bp in length. The temperature profile used for PCR amplification and subsequent determination of the nuclear-encoded LSU rDNA sequence (GenBank DQ289020) was established as described previously (Hansen et al. 2003, Hansen and Daugbjerg 2004).

Sequence alignment. The LSU rDNA sequence of *Esoptrodinium* was determined in both directions and added to the same data matrix recently compiled by Moestrup et al. (2006) to elucidate the phylogeny of woloszynskioid dinoflagellates. The data matrix analyzed here comprised a total of 40 dinoflagellates and sequences were aligned by incorporating information from secondary structure of LSU rDNA as suggested by de Rijk et al. (2000). The alignment comprised 1477 bp, including introduced gaps and covered 36 bp upstream domain D1–20 bp downstream D6 (see the secondary model for the LSU rDNA for *Prorocentrum micans* proposed by Lenaers et al. (1989)). Because of ambiguous alignment of domain D2, a fragment starting 8 bp downstream D2 to the end of this domain was omitted before phylogenetic analysis, hence leaving a fragment of 1124 bp for the analyses. The data matrix was manually edited using MacClade ver. 4.07 (Maddison and Maddison 2003).

Phylogenetic analyses. We used PAUP* ver. 4b10 (Swofford 2003) for maximum parsimony (MP) and neighbor-joining (NJ) analyses and MrBayes ver. 3.1 (Ronquist and Huelsenbeck 2003) for Bayesian analysis (BA). MP analyses were conducted with 1000 random additions in heuristic searches and a branch-swapping algorithm (tree-bisection-reconnection). All characters were equally weighted and unordered. Gap positions were treated as missing data. For MP bootstrap analyses we used 1000 replications. Modeltest ver. 3.6

(Posada and Crandall 1998) was used to search for the best model for the LSU rDNA sequences using hierarchical likelihood ration tests and the best-fit model found was TrN + I + G (Tamura and Nei 1993). Among sites rate heterogeneity was $\alpha = 0.6328$, an estimated proportion of invariable sites was $I = 0.2569$ and two substitution rate categories were A–G = 2.7815 and C–T = 6.6913. Base frequencies were set as follows A = 0.288, C = 0.1698, G = 0.2713 and T = 0.2709. The Tamura and Nei model was used to compute dissimilarity values and the resulting distance matrix was applied to build a tree with the NJ method. For NJ bootstrap we used 1000 replications. For the BA, a GTR substitution model was used with base frequencies and substitution rate matrix estimated from the data matrix. Four simultaneous Monte Carlo Markov chains (MCMC; Yang and Rannala 1997) were run from random trees for a total of 1×10^6 generations (Metropolis-coupled MCMC). A tree was sampled every 50 generations and the "burn-in" was evaluated for stationarity by examination of the plateau in log-likelihood over generations using Tracer ver. 1.2.1 by A. Rambaut & A. Drummond and an Excel spreadsheet. "Burn-in" of the chain occurred in fewer than 27,000 generations so the first 540 trees were discarded, leaving 19,461 trees for estimating posterior probabilities (PP). Thus, PP values were obtained from the 50% majority rule consensus of the kept trees. To confirm that the analysis was not trapped at a local optimum BA was performed three times (Leaché and Reeder 2002).

Outgroup species. Previous molecular studies addressing the phylogeny of major groups of eucaryotes have shown that ciliates form a sister group to dinoflagellates (van de Peer et al. 1996). Together with the Apicomplexa they constitute the alveolates. The morphological synapomorphic character is the cortical alveolae under the plasma membrane (Patterson 1999). Hence, we used two ciliates (*Tetrahymena pyriformis* and *Tetrahymena thermophila*) to root the ingroup of dinoflagellates in all phylogenetic analyses.

RESULTS

Morphology. The roughly obovoid cells were mostly 10–16 µm long and 7–11 µm wide (average of 70 cells were 11.9 and 9.2 µm, respectively), with occasional large cells about 18 µm long and 12 µm wide, and in some batches numerous tiny cells down to 8 µm long and 5 µm wide. Large cells were often seen to carry two longitudinal flagella. Most cells were slightly flattened dorsoventrally, but some were nearly circular in apical view. The cingulum was a deep and slightly descending groove that extended from the ventral face to about the mid-dorsal side, sharply delimiting on the left side of the cell the longer epicone from the shorter and narrower hypocone. The right side of the cell was almost straight or smoothly curved although some cells showed a slight depression marking the lower-right edge of the epicone (Fig. 1a). The apex was broadly rounded and the sides of the epicone were nearly straight in the longer cells, or slightly curved to the shape of a helmet in shorter ones (Fig. 1a); an inflexion near the lower-left edge of the epicone produced a beak-like projection in a few cells (not shown). The antapex was usually round, although the shape of the hypocone was more variable, especially in the smaller cells (Fig. 1, a-c). Near the proximal end of the cingulum the upper edge was somewhat raised, invading the epicone (Fig. 1b, short arrow). The transverse flagellum undulated in a relatively loose helix and did not extend significantly beyond the end of the cingulum. The sulcus was surprisingly inconspicuous given its appearance in the TEM, and it was only clearly visible in slow-moving cells in favorable positions in the light microscope. The longitudinal flagellum was usually slightly longer than the cell.

The cells swam rapidly, with velocities reaching over 200 µm/s as estimated from video recordings, and frequently changed direction. They also showed a tendency to swim in tight circles for minutes on end, especially in microscope preparations, often turning around in the same spot with their ventral or dorsal side upwards, invariably with the apex moving toward the cell's right and the longitudinal flagellum trailing around the right edge of the cell.

The cell contents were often obscured by food vacuoles, containing prey cells ranging in size from approximately 10 µm long *Chlamydomonas* cells (Fig. 1d) to chlorelloid cells some 3–6 µm in diameter; large *Esoptrodinium* cells were seen containing up to 10 food

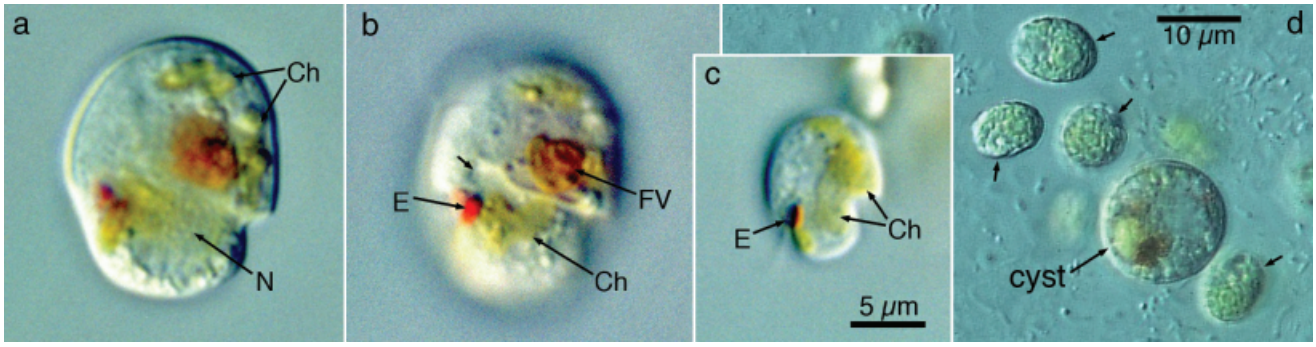

FIG. 1. Morphology of *Esoptrodinium gemma* swarmers and cyst. Differential interference light microscopy. FV, food vacuole; N, nucleus. (a, b) Ventral view of a relatively large cell in optical section (a) and in surface focus (b), showing the different-sized parts delimited by the incomplete cingulum, and the main cell structures. The short arrow in (b) indicates the proximal part of the cingulum invading the epicone. Scale bar as in (c). (c) Left-ventral view of a small cell. Note the band-shaped chloroplast (Ch) and the eyespot (E). (d) A cyst and *Chlamydomonas* cells (short arrows) from a mixed culture.

vacuoles. A red eyespot, shaped as a markedly curved plate with an outward facing concavity, was visible near the base of the longitudinal flagellum, right below the proximal end of the cingulum (Fig. 1, b and c). The nucleus was located in the upper part of the hypocone, on the left side of the cell (Fig. 1a). Although difficult to see at low magnification, closer examination always revealed the presence of one or two band-shaped, yellow-green chloroplasts (Fig. 1c), which appeared more or less broken up in cells containing food vacuoles (Fig. 1, a and b).

Round, smooth-walled cysts were found in the sediment of field-collected material and on the bottom of the culture wells, where their number increased as the cultures grew old (Fig. 1d); their cytoplasm resembled that of flagellate cells and often contained food vacuoles, but an eyespot was not seen. Cyst diameter ranged from 12 to 16 μm ($n = 15$).

Feeding. In rapidly growing cultures with plenty of food organisms most cells of *Esoptrodinium* exhibited a rapid, jerky and somewhat helical motion. Inverted microscope observations of these batches in wells of culture plates revealed the presence of concentration areas where groups of dinoflagellate cells swam around some prey cells, some distance away from other similar groups. The attracting power of some prey cells was used to increase the chances of observing feeding events at higher magnification in microchambers. The selection of such cells was dictated by the repeated approach by *Esoptrodinium* cells that remained for periods of seconds to minutes rotating with the ventral side toward the prey while moving around it, whereas nearby prey cells were not approached.

Although on most occasions the dinoflagellate cells would leave without feeding, prey ingestion was observed a few times. The ingestion process lasted in the order of 5 s and, although the cells moved more slowly while handling the prey, rotation out of the plane of focus often concealed all details. The prey cells were ingested through the ventral side of the hypocone. A wide and thin pseudopod embraced one side of the prey and drove it to the concave ventral face of the somewhat deformed dinoflagellate cell, which squirmed back to its previous shape after ingestion. The edge of the thin pseudopod was a distinctly thicker cylindrical structure 1–2 μm wide that was interpreted as a peduncle based on its appearance and position in the cell (Fig. 2).

General ultrastructure. The general fine-structural features of the cells are shown in Figures 3 and 4. The nucleus was a typical dinokaryon, extending from the flagellar base area to the left, near the ventral surface, approximately at cingulum level (Fig. 3a). Mitochondrial profiles of the usual dinoflagellate type were present in all sections, in central as well as peripheral cytoplasm (Figs. 3, a and b, and 4a). Dictyosomes were located in the central part of the cell, especially near the flagellar base area (Fig. 3a). Trichocysts were common along the surface (Figs. 3a and 4a). Starch grains and oil droplets occupied a large portion of the cytoplasm (Figs. 3, a and b, and 4a). The cells contained large food vacuoles, each apparently with a single prey cell in various degrees of degradation (Fig. 3, a and b). The plasmalemma and the underlying amphiesmal vesicles, although disrupted in some places, were intact over most of the cell surface; the vesicles tightly abutted one another and did not contain any plate-like material (Fig. 3, d and e). A thin layer of electron-opaque material (about the width of a unit membrane) covered the cytoplasmic surface of the inner membranes of the amphiesmal vesicles (Fig. 3, d and e, arrowheads). Transversely elongated vesicles underlay the peripheral microtubules along most of the surface (Figs. 3, a–d and 4a). Collared pits, about 150 nm deep and 50 nm wide in their constricted part, were very sparsely distributed on the surface (Fig. 3e).

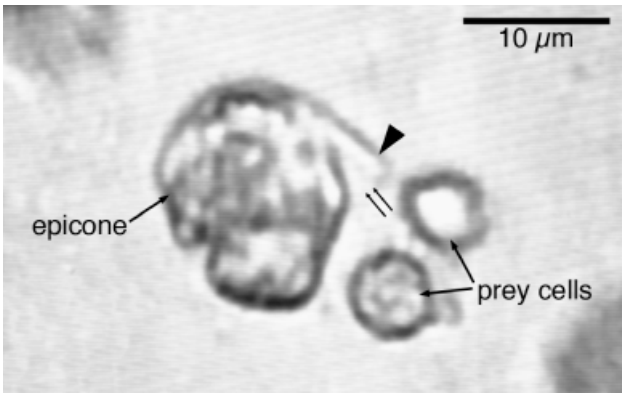

FIG. 2. *Esoptrodinium gemma* engaged in feeding (approximate dorsal view). The prey cells are chlorelloid green algae. Image taken from video recording. Note the extended peduncle (arrowhead). The double arrow indicates the position of a cytoplasmic sheet extending from the peduncle to the cell body, visible in the footage but imperceptible in the still image.

Chloroplast. Chloroplast profiles were present in all cells examined, either scattered throughout the cytoplasm (Fig. 3b) or restricted to a part of the cell (see Figs. 3a, no chloroplasts visible, and 4a, two sections of the same cell). The chloroplasts were bounded by three evenly spaced membranes and the stroma was crossed by bands of three thylakoids (Fig. 4b). Thylakoid-free areas were visible in some chloroplast lobes (Fig. 4a).

Ultrastructure of the cyst. The contents of the cyst were essentially similar to the cytoplasm of flagellate cells, with numerous starch grains and oil droplets, and some apparently old food vacuoles (Fig. 5a). Chloroplast profiles had the same appearance in the cyst as in flagellate cells (Fig. 5, a and b). A continuous wall surrounded the cyst (Fig. 5a); it was about 120 nm thick and had a homogeneous appearance except for an outermost thin layer that was more electron-opaque (Fig. 5b). Two unit membranes, parallel to each other, were found in the space

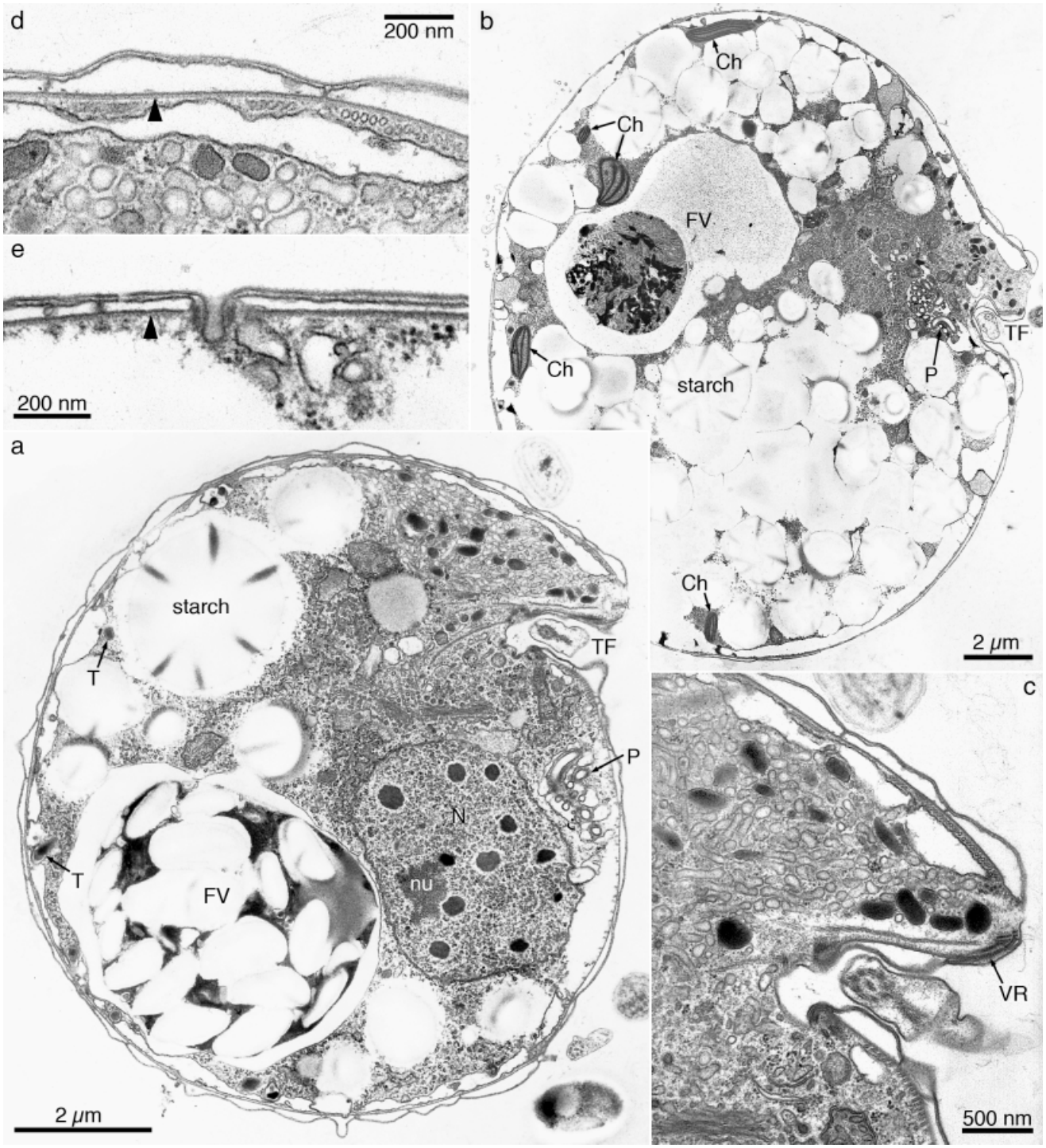

FIG. 3. *Esoptrodinium gemma*. General ultrastructure and details of the amphiesma. Ch, chloroplast; FV, food vacuole; N, nucleus; nu, nucleolus; P, pusule; T, trichocyst; TF, traverse flagellum. (a) Transverse section of a cell with a single set of basal bodies, viewed from the antapex near the exit point of the transverse flagellum. (b) Oblique-longitudinal section of a cell with a double set of basal bodies (not visible in this section), viewed from the right near the proximal end of the cingulum. (c) Ventral area of the same cell as in (a), showing the location of the feeding and flagellar apparatuses. Note the ventral ridge (VR). (d, e) Cell surface. The arrowheads indicate a layer of electron-opaque material at the cytoplasmic surface of the inner amphiesmal membrane. (e) Collared pit at the cell surface.

between the wall and the plasmalemma, which was underlain by an electron-opaque layer of about the same thickness as the membrane (Fig. 5b).

Pusule. The pusular system consisted of a long, extensively coiled tube wrapped in a vesicle; although the tube was non-ramified, in the sense that

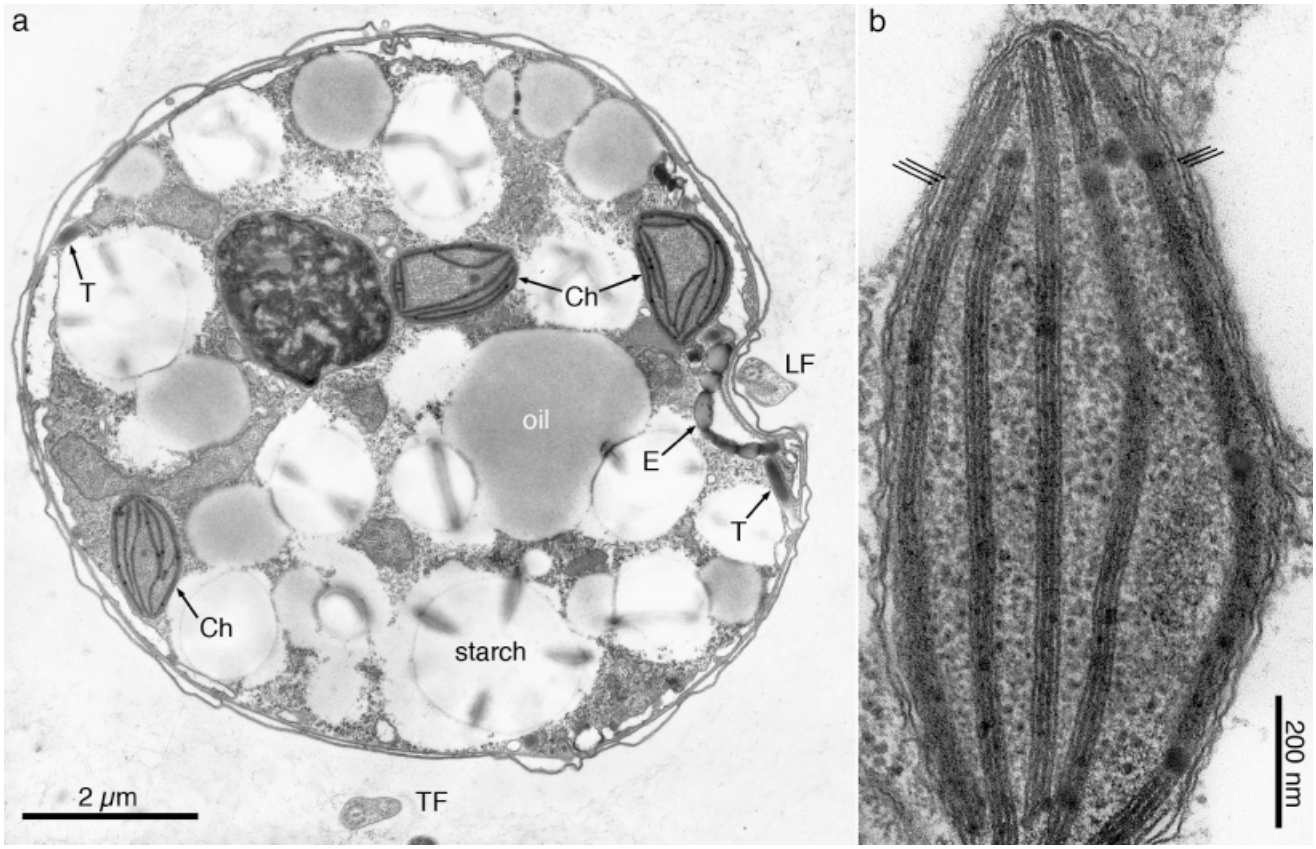

FIG. 4. *Esoptrodinium gemma*. General ultrastructure and detail of the chloroplast. LF, longitudinal flagellum; T, trichocyst. (a) Transverse section through the middle of the sulcus (antapical view, same cell as in Fig. 3a). Note the eyespot (E) underneath the sulcus, and the chloroplast lobes (Ch). (b) Chloroplast, showing three evenly-spaced bounding membranes (triple arrows).

it did not divert into long branches, much of its distal part was surrounded by numerous diverticula, each about 150 nm long, with a round distal end and a constricted connection to the main tube (Fig. 6). The width of the tube was 100–130 nm throughout its length. The inner portion of the tube contained some peripheral electron-opaque material with a granular appearance (Fig. 6). Only one pusule was found in the cells that had a single set of flagella, whereas in the cell that had a double set of basal bodies two pusular tubes were present, each tube attached to one of the two longitudinal flagellar canals (Figs. 8b and 9). No pusule was seen attached to the transverse flagellar canal.

Eyespot. The eyespot was shaped as a curved plate underlying the full width of the proximal part of the sulcus for over 2 μm (Figs. 4a, 6, and 9). It consisted of one to three layers of globules with sizes varying between approximately 100 and 380 nm; in some places the globules appeared fused together, forming a continuous layer about 100 nm thick (Figs. 6 and 10d). When two or three layers were present their middle lines were placed approximately 150 nm apart, as measured in cross-sections of the structure. Although chloroplast lobes were present near the sulcus, they were not connected to the eyespot (Figs. 4a and 6). In the cell with two longitudinal flagella two sulcal depressions were present; the shape of the underlying eyespot accompanied the shape of the depressions and some of the layers of globules were discontinuous (Fig. 9).

Flagellar apparatus. A diagrammatic view of the flagellar apparatus of a cell with two longitudinal flagella (a planozygote) is given in Figure 7. Structures associated with the longitudinal basal body (LB) of a cell with a single longitudinal flagellum are shown in Figure 8. Flagella and basal body (BB)-associated structures in the cell with a double set of basal bodies are shown in Figures 9–12, a–c. The area where the peduncle exits the cell is shown in Figure 12d and e, taken from the same series of sections as Figure 8.

The deeply marked sulcus closed into a tubular chamber near its proximal end, sheathing the longitudinal flagellum for approximately 700 nm (Fig. 8a and b); a striated collar limited the innermost part of this chamber, the longitudinal flagellar canal, which was bounded by a single membrane (Fig. 8c). In the free part of the longitudinal flagellum a fibrous rod ran alongside the axoneme. Starting at 300–400 nm from the base of the flagellum, an additional layered structure, about 300 nm wide and 20 nm thick, was placed

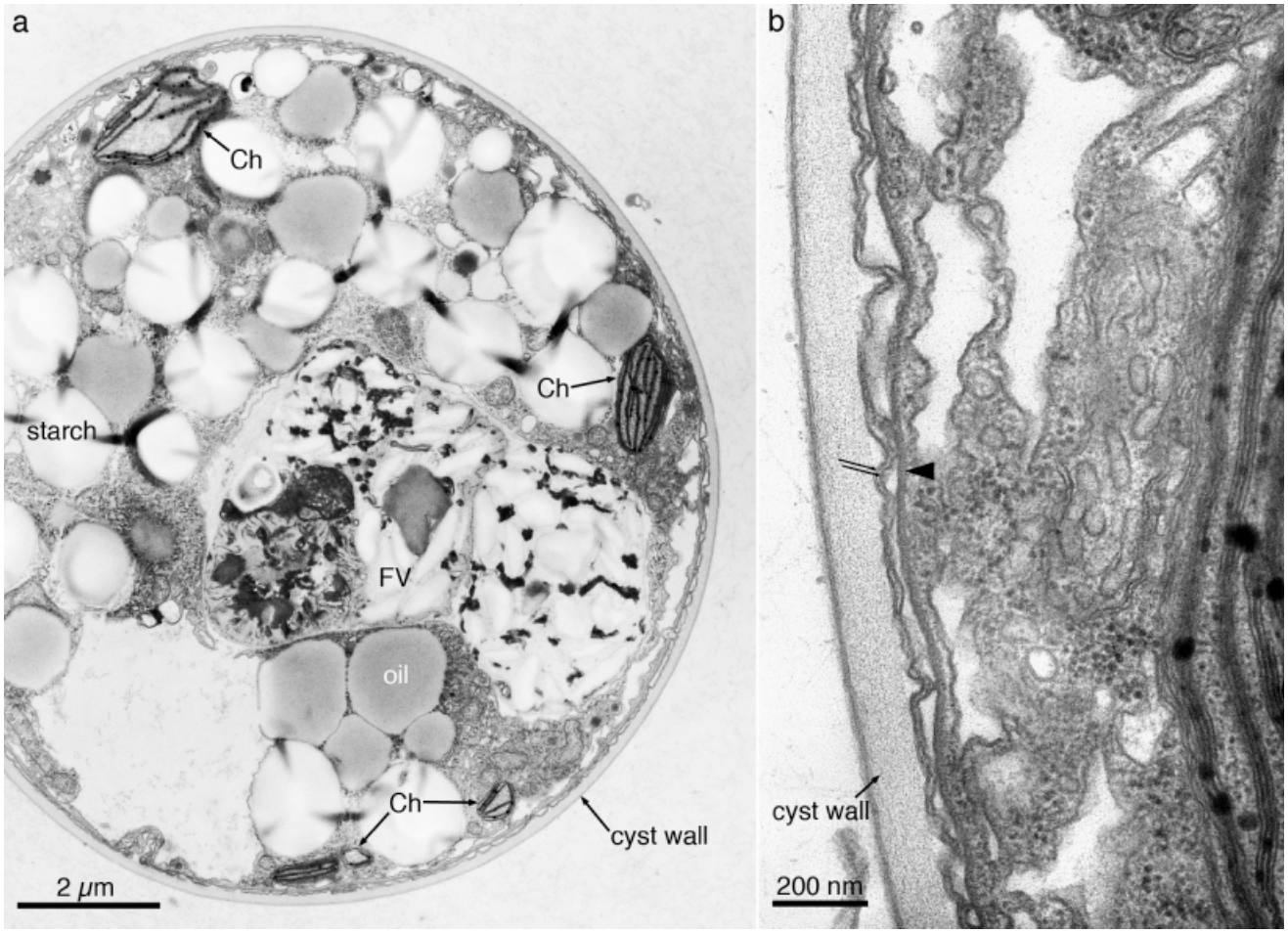

FIG. 5. *Esoptrodinium gemma* cyst. (a) General view. Note the chloroplast lobes (Ch) and the food vacuole (FV) with disorganized contents. (b) Cyst surface. Two parallel membranes (arrows) are visible between the cyst wall and the cytoplasmic membrane. The arrowhead indicates the electron-opaque layer underlying the plasmalemma. Small slanted numbers refer to the section number.

beneath the flagellar membrane on the left side of the paraxonemal rod (Figs. 8a, arrowhead; 9 and 10d). The LB was associated with a single microtubular strand, the longitudinal microtubular root (LMR; designated r_1 by Moestrup 2000). As seen in transverse sections, the distal part of the LMR consisted of approximately 25 microtubules placed along the left-dorsal side of the sulcus (Fig. 8, a and b). Near the LB the microtubules of the LMR bent in different directions whereby the structure bifurcated, with a group of six to seven microtubules arching past the dorsal side of the LB and associating with its right side (Figs. 8, e–h and 10, a–c); a striated fiber (the striated root connective, SRC) attached to the dorsal side of this right branch of the LMR, spanned the distance to the transverse basal body (TB) and attached to the proximal end of the transverse striated root (TSR) (Figs. 8, h; 10, a–c, and 11a and b). The microtubules associated with the right-dorsal side of the LB were nearly perpendicular to the BB triplets and at least one (perhaps two or three) continued on an almost reverse course toward the longitudinal flagellar canal (Fig. 8, c–h). The remaining LMR microtubules associated with the left side of the LB and continued past its proximal end on a nearly straight line for some 300 nm, their dorsal side lined with electron-opaque material (Figs. 10, b–d and 11, a–c). Several thin fibers attached to three triplets on the left-dorsal side of the TB and widened toward the ventral surface of the LMR, connecting to groups of three to five microtubules (Figs. 8, e–h and 10, a–c).

The basal bodies were inserted at an angle of approximately 135°, with the proximal end of the TB extending slightly to the right of the LB. The proximal ends of the basal bodies were approximately 250 nm apart and were not directly connected to each other (Figs. 10b and 11a). Two microtubule-containing roots were associated with the TB; the TSR, with its associated microtubule (TSRM; r_4, sensu Moestrup 2000), was attached to the dorsal-posterior face of the TB and extended for 1.2–1.5 μm along a nearly straight path toward the striated collar that delimited the transverse flagellar canal (Figs. 10, c–e; 11b and c; and 12, a–c). The transverse microtubular root (TMR; r_3, Moestrup 2000), consisting of a single microtubule surrounded

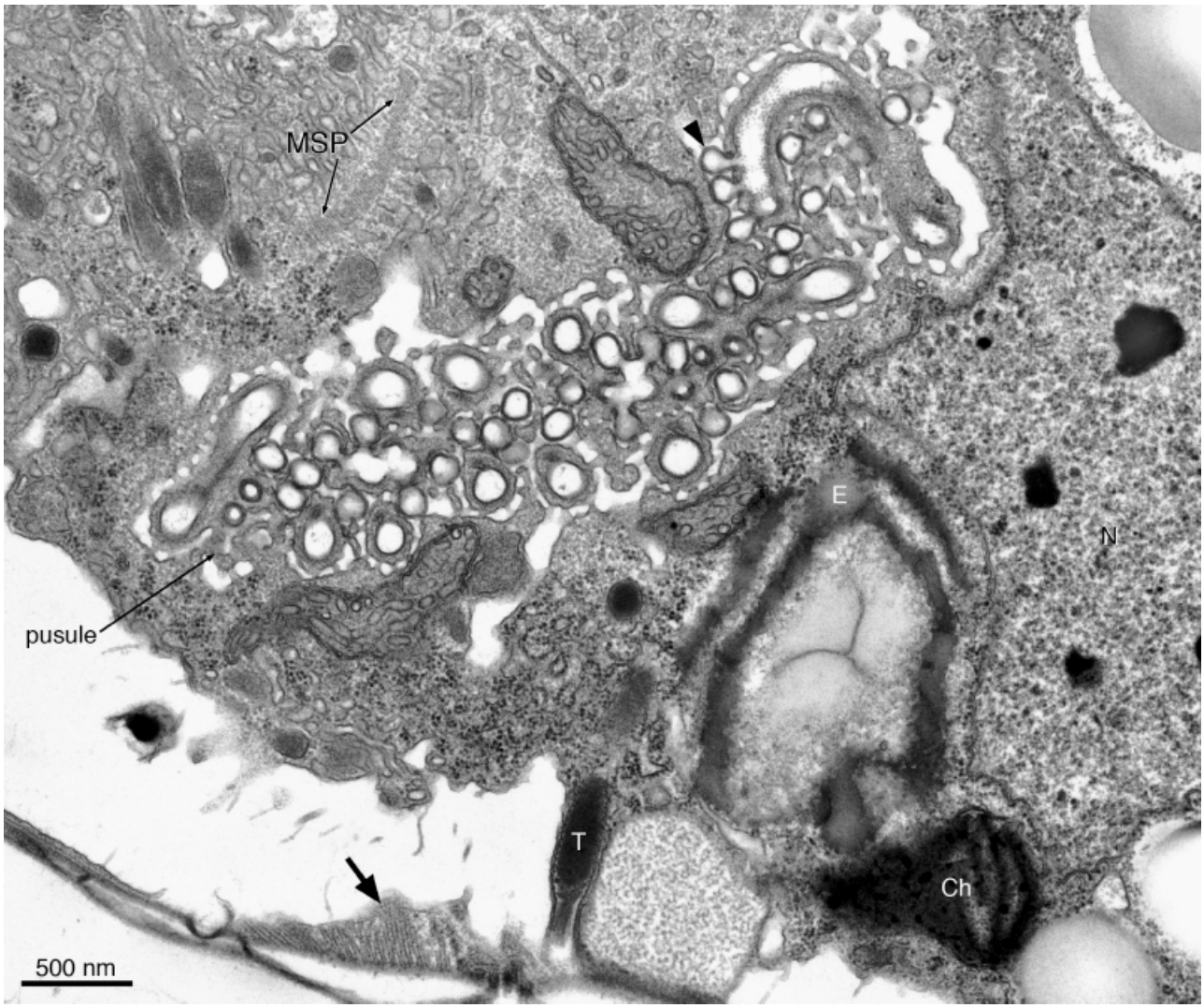

FIG. 6. *Esoptrodinium gemma*. Ventral area. Oblique-longitudinal section viewed from the ventral-left side, with the cell apex tilted some 30° toward the observer. Note the diverticula to the pusular tube (arrowhead) and a bundle of subthecal microtubules on the right side of the sulcus (thick arrow). LB, longitudinal basal body; SRC, striated root; TB, transverse basal body; TMR, transverse microtubular root; TSR, transverse striated root; TSRM, transverse striated root microtubule.

by electron-opaque material near its proximal end, attached to the anterior-dorsal side of the TB and extended for some 1.5 μm, curving around the transverse flagellar canal; starting about 600 nm from its base the TMR nucleated a row of microtubules, the TMR extension (TMRE), oriented diagonally toward the dorsal-right side of the cell for somewhat over 1 μm (Figs. 10, c–e; 11b; and 12, a and b).

Whereas each longitudinal flagellum of the cell with a double set of basal bodies exited the cell through a separate flagellar canal, the two transverse flagella converged to the same transverse flagellar canal (Fig. 11, a–c). As verified in serial sections, the transverse flagellum arising from the left set of basal bodies, as well as both longitudinal flagella, were unbroken. In contrast, the transverse flagellum originating from the right set of basal bodies terminated within the flagellar canal (Fig. 11c).

Ventral ridge and feeding apparatus. The structure herein called ventral ridge (VR) extended along the surface from the left-ventral side of the transverse striated collar toward the peduncular striated collar (PSC; see below; Figs. 3c and 12c); in its middle part it was formed by lateral well-defined fibers with a densely striated appearance in longitudinal view, connected by an area of loosely arranged thin fibrils. A bundle of orderly arranged rows of microtubules, triangular in cross-section, was present on the right side of the sulcus (Figs. 6 and 9); following the bundle through the sections it was seen to flatten out progressively as it approached the proximal end of the sulcus and continued its way toward the right side of the VR.

A small peduncle emerging from the cell is shown in Figure 12e; it was bounded by a single membrane, and a ring of fibrous material (PSC) surrounded its base. In

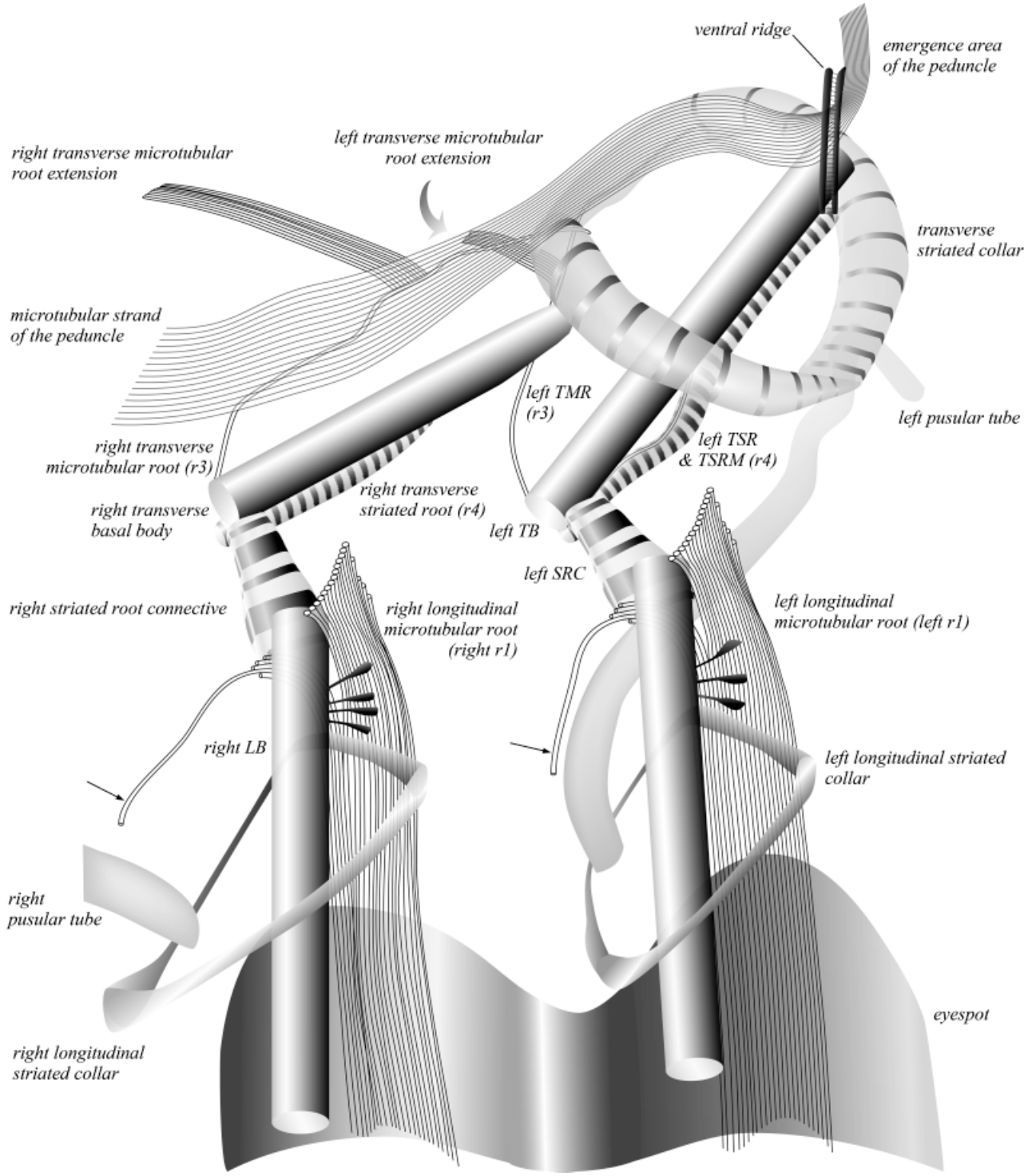

FIG. 7. Flagellar apparatus of *Esoptrodinium gemma*. Diagrammatic representation of the peduncular and flagellar base area of a planozygote in ventral view. The approximate position of the ventral ridge is shown, but the connections to the transverse striated collar were omitted. The microtubular strands are represented proportionally narrower than in the sections to avoid overcrowding the drawing; in particular, the proximal end of the left LMR lies closer to the transverse striated collar than indicated. E, eyespot; LF, longitudinal flagellum; LMR, longitudinal microtubular root; LSC, longitudinal flagellum striated collar; P, pusule; SRC, striated root connective (TSR to LMR).

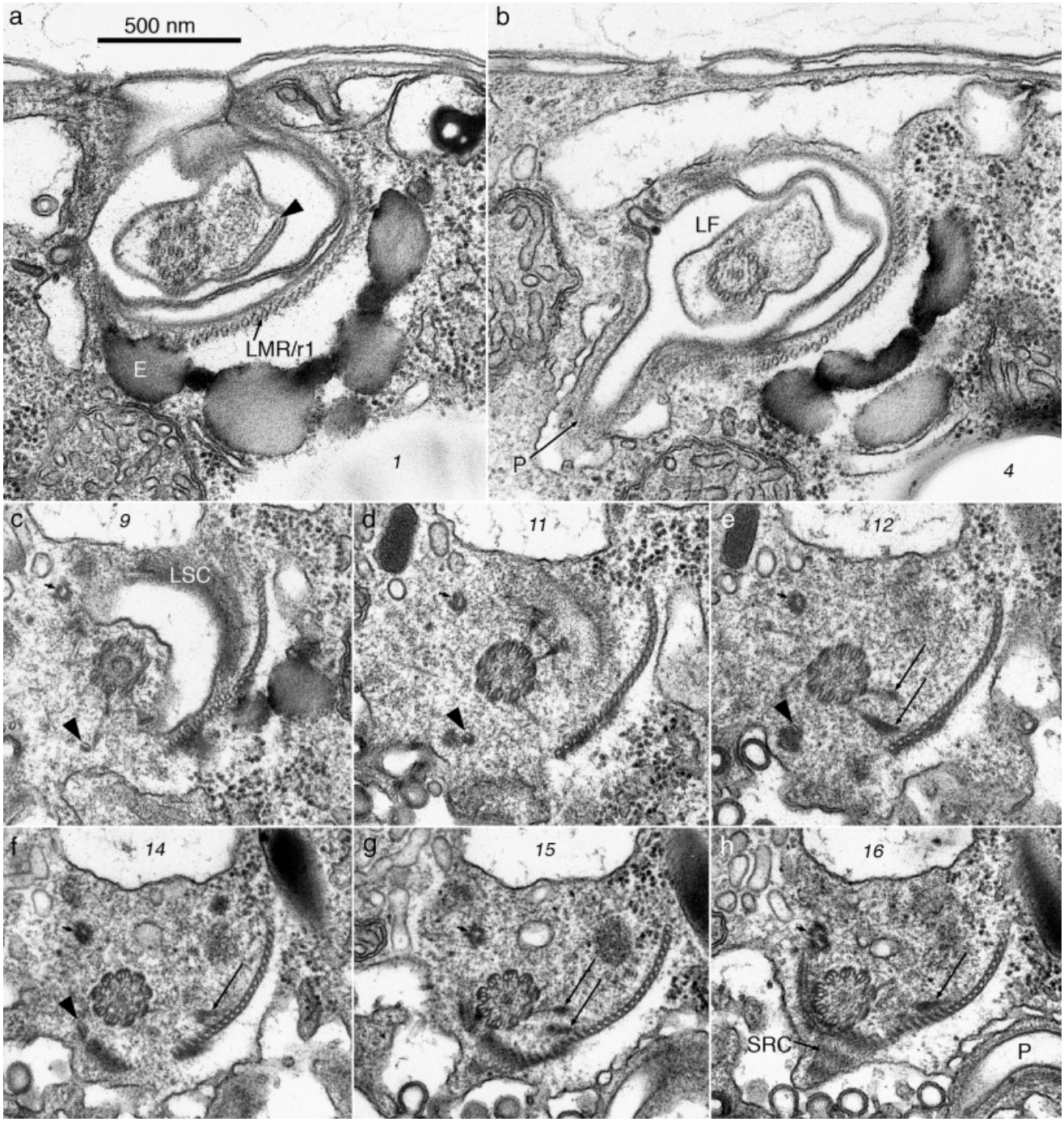

FIG. 8. *Esoptrodinium gemma*. Flagellar apparatus of a cell with a single set of basal bodies in antapical view. Non-adjacent serial sections proceeding toward the apex, showing the longitudinal flagellum and basal body (BB), and associated structures (same cell as in Figs. 3a and 4a). The sections shown in (f–h) were tilted 16° to give a vertical view of the BB. Small slanted numbers refer to the section number. The scale bar applies to all figures. E, eyespot; LF, longitudinal flagellum, LSC, longitudinal flagellum striated collar; SRC, striated root connective (TSR to LMR). (a, b) Longitudinal flagellum enclosed in a tubular chamber at the proximal end of the sulcus. Note the layered structure on the left side of the paraxonemal rod (arrowhead) and the connection of the pusular tube (P) to the longitudinal flagellar canal. (c–h) Longitudinal basal body (LB) and its association with the proximal part of the longitudinal microtudinal root (LMR). One microtubule (arrowheads) is visible diverging from the branch of the LMR that contacts the right side of the LB and continuing toward the flagellar canal. Electron-opaque material with the aspect of a hollow fiber (short arrows) approaches the right end of the LMR from the ventral side of the LB. Fibers extend from triplets of the LB to the ventral side of the LMR (arrows).

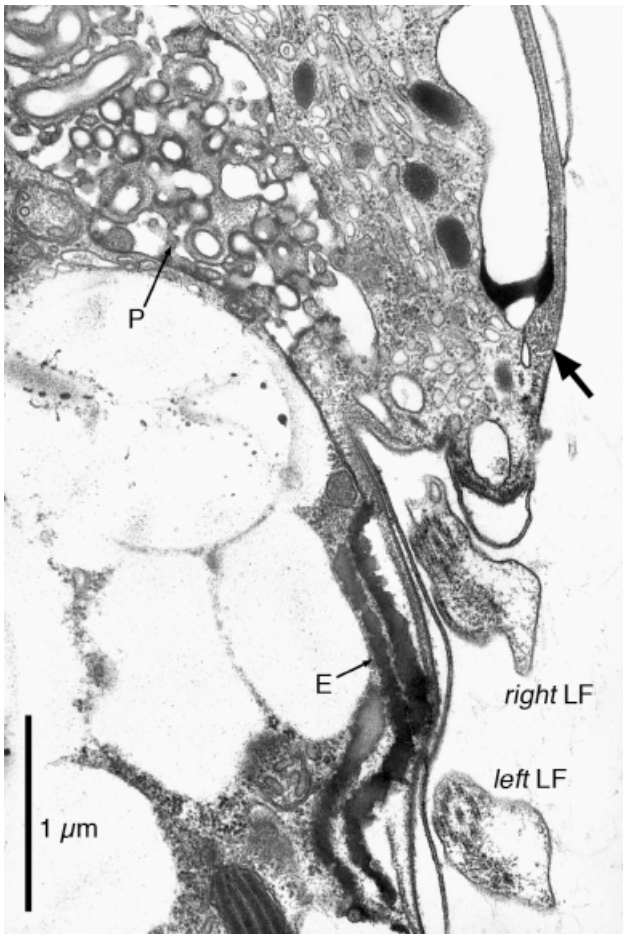

FIG. 9. *Esoptrodinium gemma*. Oblique-longitudinal view of the sulcal area of the cell with a double set of basal bodies. The two longitudinal flagella (LF) and one of the pusular tubes (P) are visible. The eyespot (E) follows the wavy shape of the two sulcal depressions. A bundle of subthecal microtubules on the right side of the sulcus is marked by a thick arrow.

serial sections, a connection could be followed from the transverse striated collar, through the VR, to the PSC, although only a very thin layer of electron-opaque material was visible in some sections. A single strand of about 30 microtubules, which was over 5 μm long in the large cell shown in Figure 3b, extended into the peduncle; this microtubular strand of the peduncle (MSP) ran nearly parallel to part of the TMRE and the two strands of microtubules were in some places less than 200 nm apart (Fig. 11b). Numerous elongate vesicles, many of which with electron-opaque contents, were present in the ventral area near the MSP.

Nucleotide divergence and phylogeny of Esoptrodinium. The phylogenetic inferences based on MP, NJ, and BA (Fig. 13) all suggest that *E. gemma* forms a sister taxon to the two species of the woloszynskioid genus *Tovellia* (viz. *Tovellia coronata* [Wołoszyńska] Moestrup, K. Lindberg et Daugbjerg and *T. sanguinea* sp. ined.). Thus, *Esoptrodinium* is recognized as the third genus in the recently proposed family Tovelliaceae (Lindberg et al. 2005). It should be noted that this family is not well supported in terms of bootstrap values in MP and NJ analyses (51% and 57%, respectively) whereas it is highly supported in terms of PP (100) from Bayesian analyses. In general the tree topology of the deep branches is not well supported in terms of bootstrap values and PP and therefore the sister group relationships of major lineages of dinoflagellates could not be established based on the nuclear encoded LSU rDNA sequences.

Estimates of the nucleotide divergence of LSU rDNA based on 1422 bp for species within the Tovelliaceae are shown in Table 1. The pairwise comparisons at the genus level are all above 20%, thus revealing a similar substitution rate within this family of dinoflagellates. However, see Lindberg et al. (2005) for a discussion on the two strains of *Jadwigia applanata* Moestrup, K. Lindberg et Daugbjerg (CCAC 0021 and FW 145).

DISCUSSION

Identity of the organism. The morphological range reported herein fits the description of the population from which the type figure of *E. gemma* was selected (Javornický 1962, 1997). Javornický (1962) found mostly colorless cells, and originally described the population as lacking chloroplasts, although the diffuse and very pale yellow–green matter found in some specimens was reinterpreted by Javornický (1997) as either chloroplasts or the remnants of ingested algae; the band-shaped structure labeled "ch?" in his Figure 1a–c (Javornický 1997, pl. 2) suggests the type of chloroplast we observed. In contrast, Thompson (1951) found "many small, diffuse, parietal, very pale yellow–green chromatophores" in all specimens but one, and this contained three large yellow to brown masses in the epicone. The observation in our material of clearly band-shaped chloroplasts in cells with no food vacuoles (see Fig. 1c) provided a basis for comparison without which the identity of the fragmented chloroplasts mixed with cell inclusions might be doubted (Fig. 1, a and b). The electron microscopical observations confirmed the narrowness of some chloroplast bands. It is interesting to note that all cells of the mirror-symmetrical *B. bernardinense* from Rügen Island had greenish–yellow chloroplasts (Javornický 1997).

Whereas Javornický (1962) described an eyespot similar to what we found, Thompson (1951) reported instead a dark spot produced by the sharp margins of the deep longitudinal flagellar pore. Interestingly, in the original description of *B. bernardinense*, Chodat (1924) mentions hematochrome granules, which he interpreted as foreign bodies and not a true eyespot, and his drawings show a dark spot in an analogous position to the eyespot of *Esoptrodinium*.

The similarities between *B. bernardinense* and *E. gemma* extend to the swimming mode observed in the population we studied, in particular the lengthy rota-

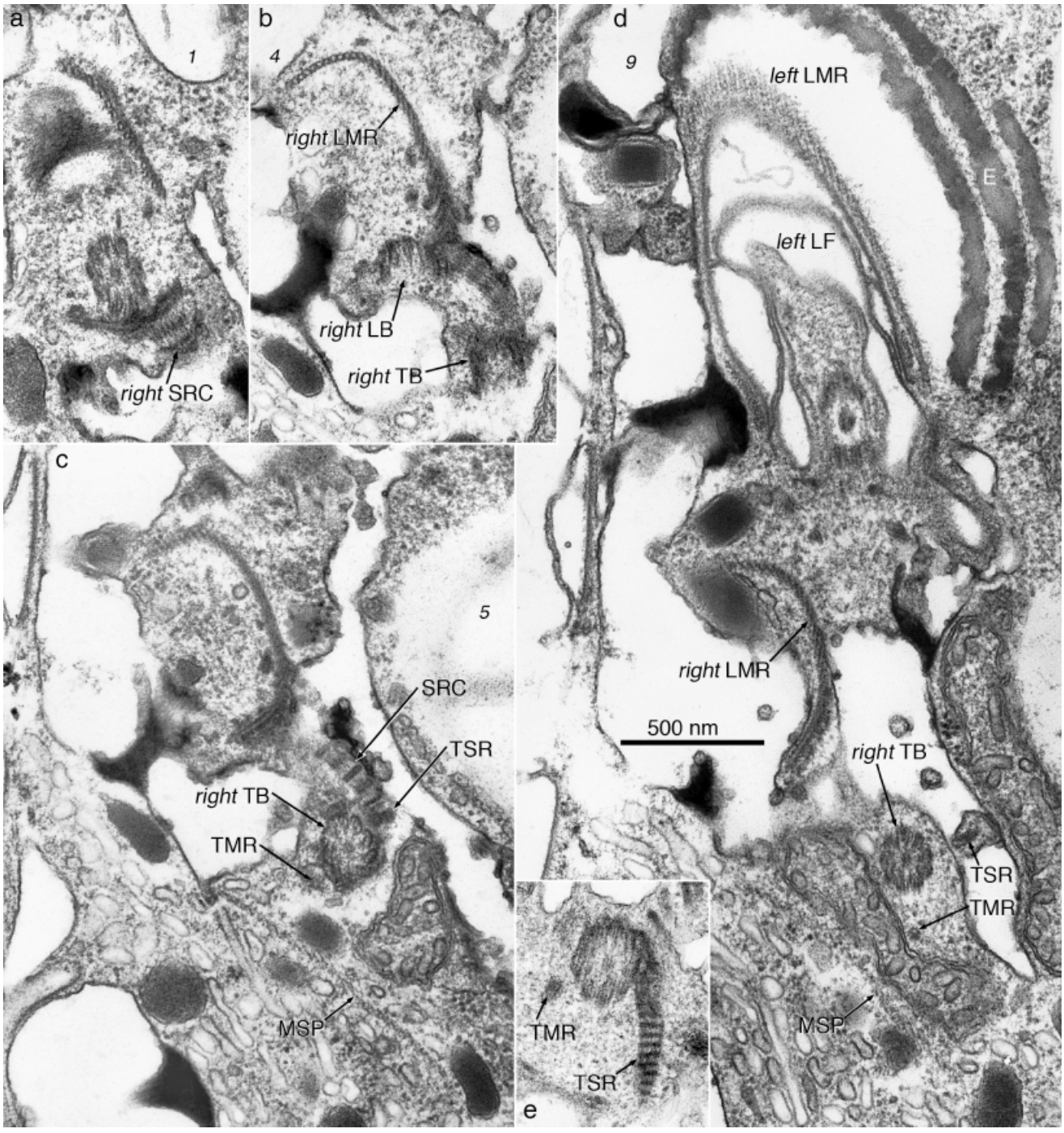

FIG. 10. *Esoptrodinium gemma*. Flagellar apparatus of the cell with a double set of basal bodies. Non-adjacent serial sections progressing from right to left. The cell is viewed from the right, with the apex tilted about 40° away from the observer. The series is presented with the sulcus oriented to the top of the images to facilitate comparison with Fig. 8. Small slanted numbers refer to the section number. The scale bar applies to all figures. See text for description.

tion on one spot, which would be adequately described as "tournant sans cesse dans un même sens, c'est-à-dire selon une ligne qui va du sommet de la moitié plus petite vers le sillon" (Chodat 1924, p. 41); four of Chodat's (1924) drawings show cells with the longitudinal flagellum around the non-indented lateral margin, the same general appearance we found in rotating specimens.

The nearly perfect symmetry between *Bernardinium* and *Esoptrodinium*, and the uniqueness of a right-oriented transverse flagellum in *Bernardinium*, are indeed surprising and the possibility of a mistake must be ad-

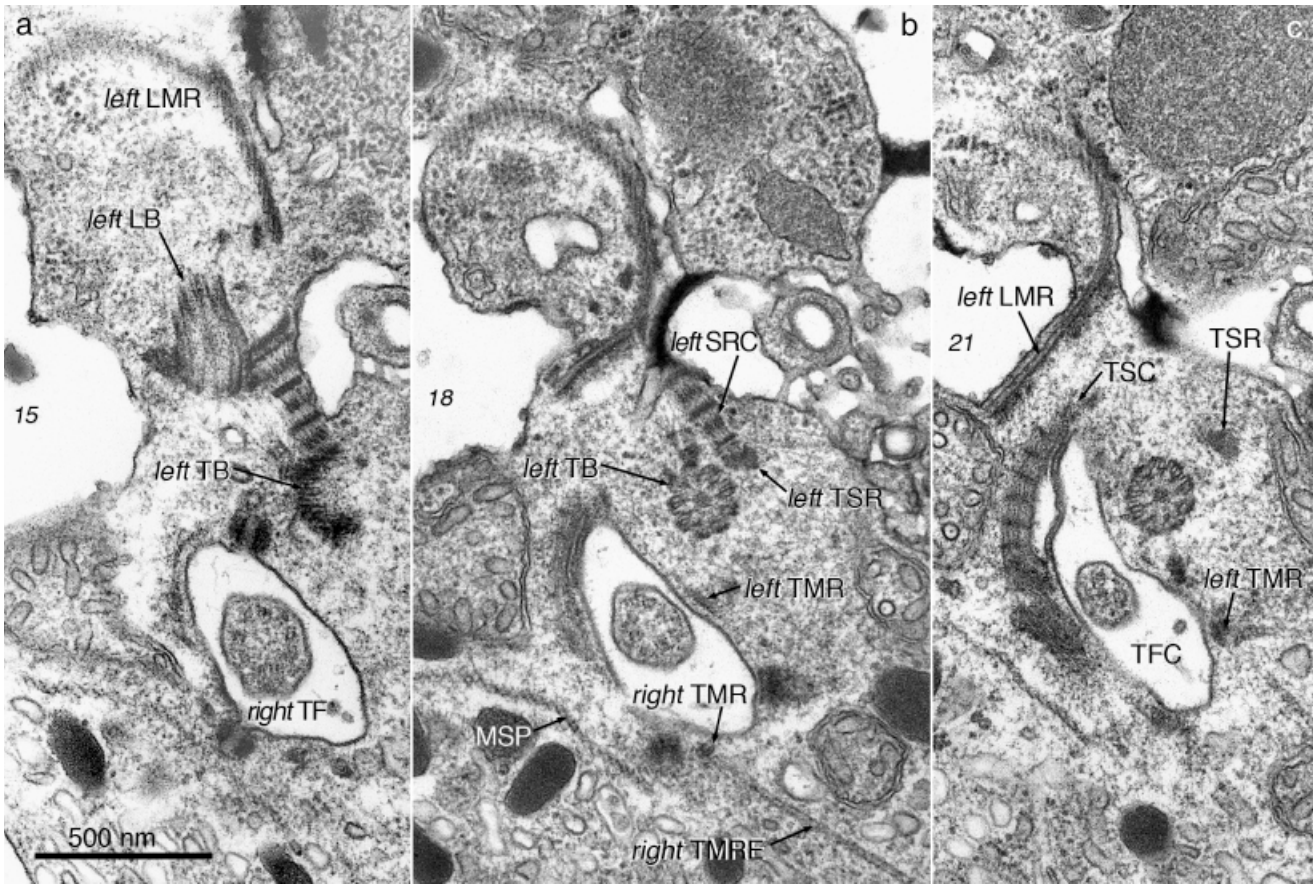

FIG. 11. Flagellar apparatus of *Esoptrodinium gemma*. Continuation of the series shown in Fig. 10. Small slanted numbers refer to the section number. The scale bar applies to all figures. See text for description.

dressed. The image formed by a traditional light microscope, with the ocular directly aligned with the objective, is rotated 180°, but it is not flipped; this means that looking through the ocular the image is seen with the same chiral orientation as the object. In contrast, inverted microscopes introduce a number of reflections and changes in viewpoint, each of which produces a mirror-symmetrical version of the previous image, the end result depending on the number of such inversions. Some years ago, while attempting to document feeding with a Leitz Labovert FS inverted microscope, we recorded on video some would-be mirror-symmetrical cells of *Prosoaulax lacustris* (F. Stein) Calado et Moestrup. As not all inverted microscopes produce mirror images (e.g. the older Wild M40 does not) a microscopist may be caught off guard against such a possibility. Javornický (1997) studied live material collected in northeast Germany and one may speculate that he observed the organism with some microscope unfamiliar to him, obtained in a nearby laboratory. We could not confirm this possibility, however, and therefore have no ground to assume a mistaken observation.

Whereas the eventual rediscovery of a *Bernardinium*-like organism with a right-oriented transverse flagellum would prove its existence, the possibility of it being the product of erroneous observations may be difficult, if not impossible, to demonstrate. As the characteristics associated with the name *E. gemma* are clearly defined, as opposed to the ambiguity inherent to the different uses of the name *B. bernardinense*, the use of the former name for the organisms we report on seems the best option.

Feeding. The clusters of rapidly swimming *Esoptrodinium* cells observed in dense mixed cultures, and the attractive power of some prey cells, betray a chemosensory system for detection of food items, although it was not clear from the observations what features characterized attractive cells. In so-called histophagous species such as *Gymnodinium fungiforme* Anisimova (= *Katodinium fungiforme* [Anisimova] Fott ex A.R. Loeblich) and *Peridiniopsis berolinensis* (Lemmermann) Bourrelly, chemosensitivity is used to find injured or dying prey; it is accurate to the point of directing the predators to the exact areas on the surface of prey where ingestible contents may flow out. These species take up food by suction through a feeding tube and, except for small items that may be taken up whole, ingest only part of their prey (Spero 1982, 1985, Calado and Moestrup 1997, see Hansen and Calado 1999, for a review). Detection of prey cells in poor physiological

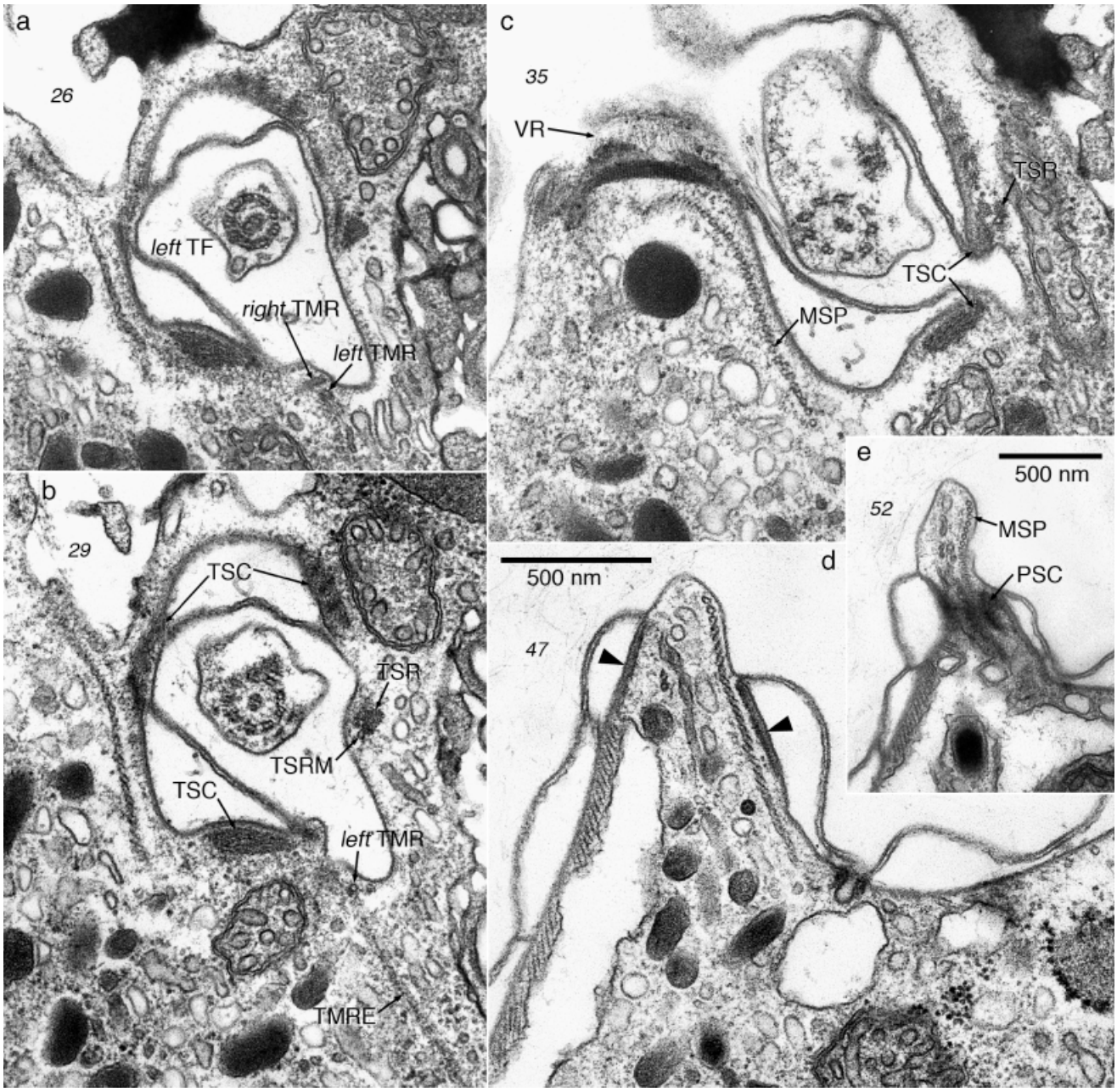

FIG. 12. *Esoptrodinium gemma*. Transverse flagellum, ventral ridge (VR) and microtubular strand of the peduncle (MSP). (a–c) Continuation of the series shown in Figures 10 and 11. Scale bar as in (d). (d, e) Same series as Fig. 8. Small slanted numbers refer to the section number. Note the thin layer of electron-opaque material (arrowheads) that connects the peduncular striated collar (PSC) to the VR.

condition, perhaps easier to capture or more digestible, may be speculated as the function of chemosensitivity in *Esoptrodinium*.

Although the rotating motion of *Esoptrodinium* cells near potential prey closely resembled the spinning displayed by *P. berolinensis* before attachment to food particles (Calado and Moestrup 1997), the emission of an attachment filament was never observed. The continuous motion of the cells throughout the engulfment process constantly shifted the observation point of view, giving rise to different appearances often difficult to interpret. Dangeard's (1892) account of food uptake in *Katodinium vorticella* (F. Stein) A.R. Loeblich (as *Gymnodinium vorticella* F. Stein) aptly describes what was visible during some observations on feeding *Esoptrodinium* cells. The few feeding events recorded on video that show the cell in focus for most of the process, combined with the ultrastructural information, suggest the involvement of the peduncular microtubules in driving forward the wide, thin pseudopod. The presence of a single membrane, not underlain by amphiesmal vesicles, extending down from the pedun-

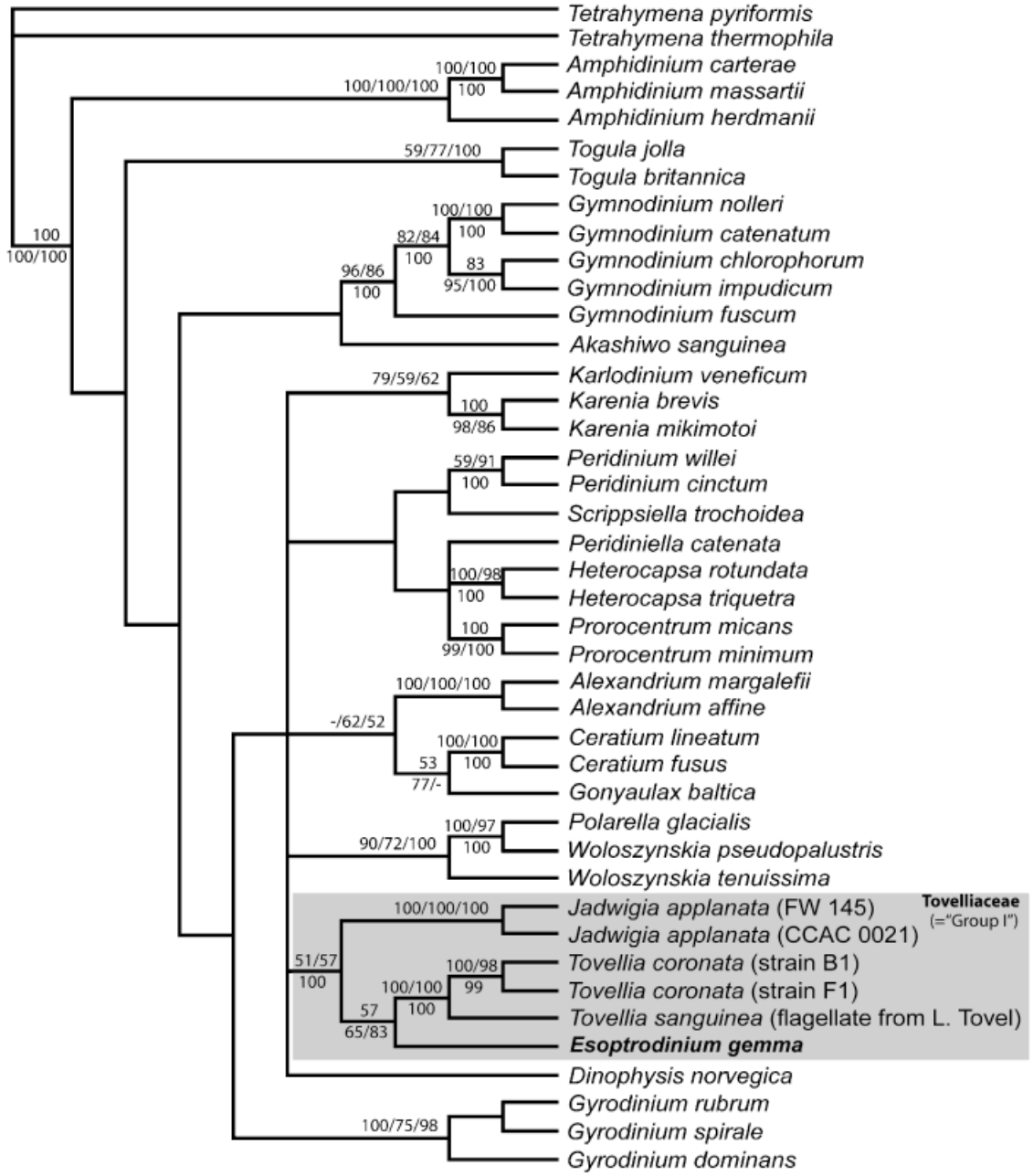

FIG. 13. Phylogeny of *Esoptrodinium gemma* inferred from unweighted parsimony analysis based on 1124 bp of nuclear-encoded LSU rDNA. Of the characters included 540 were parsimony informative and the parsimony analyses produced three equally parsimonious trees each 2632 steps ($CI = 0.436$, $RI = 0.543$). The tree topology illustrated is a strict consensus of the three parsimonious trees. Bootstrap values or support from posterior probabilities (PP) of 50% or above are written to the left of internal nodes. The first numbers are from parsimony analyses (1000 replications, characters unweighted), the second numbers are from neighbor-joining analyses based on the maximum likelihood settings obtained using Modeltest (TrN + I + G model and with 1000 replications). The third numbers are PP from Bayesian analyses and based on 19,461 trees. The two ciliates assigned to *Tetrahymena* comprised the outgroup. The family Tovelliaceae (woloszynskioid group I sensu Lindberg et al. 2005), including *Esoptrodinium*, is marked.

cle along the axis of the VR, highlights this area as the potential place of ingestion, thereby suggesting a function for this enigmatic structure.

As seen with the EM, the peduncle and associated structures of *E. gemma* are essentially similar to what was found in *Prosoaulax lacustris* (as *Amphidinium lacustre* F. Stein non auctt.; Calado et al. 1998, Calado and Moestrup 2005). However, in *P. lacustris* food is ingested through a narrower area, which was interpreted as the place of emergence of the peduncle based on its location in the cell. The apparent peduncle-assisted pseudopod formation and direct engulfment in *Esoptrodinium* illustrate a different use for the same cell structures.

TABLE 1. Sequence divergence in percentage of three genera within the Tovelliaceae (*Esoptrodinium*, *Tovellia*, and *Jadwigia*) based on 1422 unambiguously aligned LSU rDNA nucleotides

	Esoptrodinium gemma	*Tovellia coronata*	*Tovellia sanguinea*	*Jadwigia applanata* (CCAC0021)	*Jadwigia applanata* (FW145)
E. gemma	–	25.79	27.87	23.67	22.23
T. coronata	32.03	–	11.85	22.5	22.35
T. sanguinea	35.33	12.98	–	23.87	23.84
J. applanata (CCAC0021)	28.84	27.05	29.02	–	10.45
J. applanata (FW145)	26.66	26.92	28.53	11.37	–

Uncorrected distances ("*p*" values in PAUP*) are given above the diagonal and distance values calculated using Kimura 2-parameter model are given below the diagonal.

LSU, large subunit.

Morphology and ultrastructure. The cells of *E. gemma* displayed the general ultrastructural features typical of dinoflagellates. Chloroplast organization was of the usual peridinin-containing type, although the color perceived with the light microscope hints at a different pigment composition. However, the high proportion of prey cells in the mixed cultures and the small volume of the batches precluded pigment analysis of the dinoflagellate. Judging from their ultrastructural integrity, the chloroplasts seemed functional, although their relatively small size and the presence of food vacuoles in nearly all cells suggest that phagotrophy is the essential mode of nutrition. All attempts to grow *Esoptrodinium* without food organisms were unsuccessful.

The eyespot of *Esoptrodinium* belongs to Dodge's (1984) type A and to the "*Woloszynskia coronata* type" of Kawai and Kreimer (2000), and is characteristic of the family Tovelliaceae (Lindberg et al. 2005). The presence of a similar type of eyespot in *Katodinium campylops* (T.M. Harris) A.R. Loeblich (Wilcox 1989) indicates a close affinity with members of the Tovelliaceae. As seen with the light microscope, the closely related *K. vorticella* is strongly reminiscent of *Esoptrodinium*, both for the appearance of the eyespot and for the general structure of the cell; in addition, it produces a resting cyst with paracingulum and two axial horns (unpublished observations), the same type of cyst produced by *T. coronata* (Wołoszyńska 1917, as *Gymnodinium coronatum* Wołoszyńska; Lindberg et al. 2005), suggesting that the group of *K. vorticella*-related species are members of the Tovelliaceae. However, the type species of *Katodinium*, *K. nieuportense* (W. Conrad) Fott, is a poorly known marine species with a rather different appearance (Conrad 1926), possibly unrelated to most species currently assigned to *Katodinium*.

With its numerous diverticula, the pusular tube of *E. gemma* most closely resembles that of *T. coronata*, although the distal part of the tube appears somewhat more irregular in the latter species (Crawford and Dodge 1971, Figs. 13, 14; Lindberg et al. 2005, Figs. 28, 30). As in vegetative cells of *E. gemma*, a single pusule was reported in *T. coronata*, attached to the longitudinal flagellar canal (Lindberg et al. 2005). A single tubular pusule per cell was also found in *Prosoaulax lacustris*, either attached to the longitudinal or to the transverse flagellar canal (Calado et al. 1998). As the number of cells of *E. gemma* examined was small, the possibility that the pusular tube may in some cells associate with the transverse flagellar canal cannot be excluded.

Electron-opaque material with a layered appearance lining the dorsal surface of the proximal stretch of LMR has been reported from *K. campylops* and *Woloszynskia pascheri* (Suchlandt) Stosch (Wilcox 1989), two species closely related to the wolozynskioids. The relatively wide strand of nearly straight microtubules extending past the LB in *K. campylops* is similar to what we found in *Esoptrodinium*, and can also be seen in the published micrographs of *Tovellia* sp. (as *Woloszynskia* sp.; Roberts and Timpano 1989, Lindberg et al. 2005) and *J. applanata* (as *Woloszynskia limnetica* Bursa; Roberts et al. 1995). A similar arrangement is suggested in Figure 34 of Lindberg et al. (2005) for *T. coronata*. In all these species the SRC is relatively wide and attaches to the LMR near the area where the microtubules bend toward the antapex.

A bifurcating LMR, such as the one found in *Esoptrodinium*, has not been previously reported. The microtubule that extends beyond the right side of the LB is potentially confusing because this is the position where the so-called single-stranded microtubular root (SMR, usually interpreted as r_2; Moestrup 2000) is found in gonyaulacoids and peridinioids; however, the SMR has its proximal end on the right ventral side of the LB and extends in an arc in a dorso-antapical direction (see Hansen and Moestrup 1998a, Calado et al. 1999, Calado and Moestrup 2002) whereas in *Esoptrodinium* the right hand side microtubule extends from the right-dorsal side of the LB toward the ventral-right. The continuity of the projecting microtubule with the LMR was best observed in sections perpendicular to the LB (Fig. 8h) and may be difficult to perceive in other angles. Although the viewpoints of the series of sections shown in Roberts et al. (1995) are not appropriate to reveal such an arrangement, it should be noted that the conformation of the LMR schematically shown in Figure 7 fits what is visible in *J. applanata* in Roberts et al. (1995, Figs. 35–38), assuming that the structure marked by an arrowhead (in Fig. 38) is a microtubule. More detailed work on the flagellar apparatus of members of the Tovelliaceae is

needed to verify if a bifurcating LMR is a shared feature in this group. It is not clear if the SMR and the projecting microtubule of *Esoptrodinium* are homologous structures.

Organization of the planozygote. The unequivocal establishment of sexual reproduction in dinoflagellates is usually credited to Stosch (1964, 1965), who later established the identity of cells with paired longitudinal flagella as planozygotes (Stosch 1973). This has since been confirmed in numerous life cycle studies (Pfiester 1984). The generally large-sized cells found with paired longitudinal flagella in our batches of *Esoptrodinium* and the thick-walled resting cysts that abounded in older batches are recognizable, respectively as the planozygote and the hypnozygote stage in the life cycle of this species. The first published illustrations of the parallel arrangement of basal bodies and roots in a dinoflagellate are in Leadbeater and Dodge (1967a, Fig. 3) and Leadbeater and Dodge (1967b, Figs. 13, 18), showing what was interpreted at the time as recently divided pairs of flagellar bases in *Karlodinium micrum* (B. Leadbeater et J. D. Dodge) J. Larsen (as *Woloszynskia micra* B. Leadbeater et J.D. Dodge); it is now clear that the cells illustrated were planozygotes (Bergholtz et al. 2006).

In a study of flagellar transformation in *Prorocentrum micans* Ehrenberg it has been shown that the newly formed basal bodies are not parallel to the parental pair and that the parental TB develops into a LB during cell division (Heimann et al. 1995). A large angle was demonstrated in *Peridinium cinctum* (O.F. Müller) Ehrenberg between the parental and the newly formed basal bodies, which were both oriented toward the apex of the cell (Calado et al. 1999). Similarly located accessory basal bodies were shown in *Peridiniella catenata* (Levander) Balech (Hansen and Moestrup 1998b, Figs. 14–16). Parallel arrangements of basal bodies and roots have been shown in planozygotes of *Peridiniopsis berolinensis* (Wedemayer and Wilcox 1984, Figs. 19 and 20), *Scrippsiella minima* X. Gao et J. D. Dodge (Gao et al. 1989, Figs. 7 and 8; as *Scrippsiella* sp., see Gao and Dodge 1991) and *T. coronata* (Lindberg et al. 2005, Figs. 33 and 34).

We found a similar arrangement of flagellar bases and associated structures in both left and right pairs of basal bodies in the planozygote, and it was essentially the same as seen in vegetative cells; namely the roots and connectives associated with each pair of basal bodies were the same. However, it is interesting to note that not all structures in the ventral area were doubled. Whereas each longitudinal flagellar canal was connected to an independent pusular system, the eyespots were partially fused, although two longitudinal grooves were maintained. A single peduncle and MSP were present in the planozygote, associated with a single VR, in a similar position relative to the left pair of BBs as the one found in vegetative cells. Unexpectedly, we found that both transverse flagella converged to the same flagellar canal, in contrast with the two independent longitudinal flagellar canals. As seen in Figure 7, the structures that are not doubled in the planozygote (i.e. transverse flagellar canal, VR, emergence point of the peduncle; also the triangular array of microtubules on the right side of the sulcus not shown in Fig. 7) are nearly aligned longitudinally and it may be speculated that this axial area is pivotal in the rearrangements taking place during gamete fusion, because the two gametal flagellar systems seem to converge in this zone. However, the mechanisms driving the migration of some structures and the loss of others during the final stages of gamete fusion are unknown.

Although occasionally reported with two transverse flagella (Coats et al. 1984), planozygotes are more often seen with a single flagellum in the cingulum (Stosch 1973, Gao et al. 1989). Convergence to a single flagellar pore may perhaps render more difficult the retention of both transverse flagella in *Esoptrodinium*. Examination of planozygotes of other species is necessary to determine whether the organization described herein is shared by other dinoflagellates.

Phylogenetic affinities. The close affinity between *E. gemma* and the genera *Tovellia* and *Jadwigia* is strongly indicated by both the molecular data used and the general similarities in eyespot, flagellar apparatus and pusule construction, and *Esoptrodinium* is therefore assigned to the family Tovelliaceae. In contrast, the recently investigated *Woloszynskia halophila* (Biecheler) Elbrächter et Kremp contains a brick-like eyespot and has closer affinities with a group of species which includes symbiotic forms and the marine polar genus *Polarella* Montresor, Procaccini et Stoecker (Kremp et al. 2005). Interestingly, no plate material was found in *E. gemma*, a feature that would dictate its assignment to the Gymnodiniaceae in traditional taxonomical schemes. The value of amphiesmal vesicle contents as a phylogenetic marker is, however, rather uncertain as some gymnodinioids (including the type species of *Gymnodinium*, *G. fuscum* [Ehrenberg] F. Stein; Dodge and Crawford 1969, Hansen et al. 2000) have thin plates. One feature found in *Tovellia* and in *Jadwigia* that was not seen in *E. gemma* is the apical line of narrow plates; fixations for SEM were tried, but their quality was not good enough to ascertain whether this character is present or missing in *Esoptrodinium*.

Although in the phylogenetic tree shown in Figure 13 *E. gemma* is grouped with *Tovellia*, we consider that the relationship between the genera included in the Tovelliaceae is not well supported in terms of bootstrap values and posterior probability, and the available morphological characters suggest different affinities. Whereas general morphology seems closer between *Tovellia* and *Jadwigia*, the pusular tube of *J. applanata,* not shown to possess diverticula, would argue for a closer relationship between *Tovellia* and *Esoptrodinium*. On the other hand, the round cyst of *E. gemma* is more similar to the cyst of *J. applanata* than to the horned type cyst of *T. coronata*. A detailed analysis of the flagellar base area of *T. coronata* is needed to provide other characters for comparison between the genera.

A. J. C. was supported by the European Community's programme "Improving the Human Research Potential and the Socio-Economic Knowledge Base" (through Copenhagen Biosystematics Centre [COBICE]). Financial support was also provided by the Danish Science Research Council (Grant no. 21-02-0539) to Ø. M. and N. D. Prof. Jorge Rino first brought our attention to the organism on the sidewalk and kindly provided the light micrographs for Figure 1, a–c.

Bergholtz, T., Daugbjerg, N., Moestrup, Ø. & Fernández-Tejedor, M. (in press). On the identity of *Karlodinium veneficum* and description of *Karlodinium armiger* sp. nov., based on light and electron microscopy, nuclear-encoded LSU rDNA and pigment composition. *J. Phycol*. 42:170–93.

Calado, A. J., Craveiro, S. C. & Moestrup, Ø. 1998. Taxonomy and ultrastructure of a freshwater, heterotrophic *Amphidinium* (Dinophyceae) that feeds on unicellular protists. *J. Phycol.* 34:536–54.

Calado, A. J., Hansen, G. & Moestrup, Ø. 1999. Architecture of the flagellar apparatus and related structures in the type species of *Peridinium*, *P. cinctum* (Dinophyceae). *Eur. J. Phycol.* 34:179–91.

Calado, A. J. & Moestrup, Ø. 1997. Feeding in *Peridiniopsis berolinensis* (Dinophyceae): new observations on tube feeding by an omnivorous, heterotrophic dinoflagellate. *Phycologia* 36: 47–59.

Calado, A. J. & Moestrup, Ø. 2002. Ultrastructural study of the type species of *Peridiniopsis*, *Peridiniopsis borgei* (Dinophyceae), with special reference to the peduncle and flagellar apparatus. *Phycologia* 41:567–84.

Calado, A. J. & Moestrup, Ø. 2005. On the freshwater dinoflagellates presently included in the genus *Amphidinium*, with a description of *Prosoaulax* gen. nov. *Phycologia* 44:112–9.

Chodat, R. ("avec la collaboration de M. J. Zender") 1924. Algues de la région du Grand Saint-Bernard. III. *Bull. Soc. Bot. Genève Ser. 2* 15:33–48.

Coats, D. W., Tyler, M. A. & Anderson, D. M. 1984. Sexual processes in the life cycle of *Gyrodinium uncatenum* (Dinophyceae): a morphogenetic overview. *J. Phycol.* 20:351–61.

Conrad, W. 1926. Recherches sur les flagellates de nos eaux saumâtres. 1e partie: dinoflagellates. *Arch. Protistenk*. 55: 63–100, pls 1, 2.

Conrad, W. 1939. Notes protistologiques. IX. Sur trois Dinoflagellates de l'eau saumâtre. *Bull. Mus. R. Hist. Nat. Belg*. 15:1–10.

Crawford, R. M. & Dodge, J. D. 1971. The dinoflagellate genus *Woloszynskia*. II. The fine structure of *W. coronata*. *Nova Hedwigia* 22:699–719.

Dangeard, P.-A. 1892. La nutrition animale des Péridiniens. *Botaniste* 3:7–27, pls 1, 2..

de Rijk, P., Wuyts, J., van der Peer, Y., Winkelmans, T. & de Wachter, R. 2000. The European large subunit ribosomal RNA database. *Nucleic Acids Res.* 28:117–8.

Dodge, J. D. 1984. The functional and phylogenetic significance of dinoflagellate eyespots. *BioSystems* 16:259–67.

Dodge, J. D. & Crawford, R. M. 1969. The fine structure of *Gymnodinium fuscum*. *New Phytol.* 68:613–8.

Gao, X. & Dodge, J. D. 1991. The taxonomy and ultrastructure of a marine dinoflagellate, *Scrippsiella minima* sp. Nov.. *Br. Phycol. J.* 26:21–31.

Gao, X., Dodge, J. D. & Lewis, J. 1989. An ultrastructural study of planozygotes and encystment of a marine dinoflagellate, *Scrippsiella* sp.. *Br. Phycol. J.* 24:153–65.

Hansen, P. J. & Calado, A. J. 1999. Phagotrophic mechanisms and prey selection in free-living dinoflagellates. *J. Eukaryot. Microbiol*. 46:382–9.

Hansen, G. & Daugbjerg, N. 2004. Ultrastructure of *Gyrodinium spirale*, the type species of *Gyrodinium* (Dinophyceae), including a phylogeny of *G. dominans*, *G. rubrum* and *G. spirale* deduced from partial LSU rDNA sequences. *Protist* 155:271–94.

Hansen, G., Daugbjerg, N. & Franco, J. M. 2003. Morphology, toxin composition and LSU rDNA phylogeny of *Alexandrium minutum* (Dinophyceae) from Denmark, with some morphological observations on other European strains. *Harmful Algae* 2:317–35.

Hansen, G. & Moestrup, Ø. 1998a. Fine-structural characterization of *Alexandrium catenella* (Dinophyceae) with special emphasis on the flagellar apparatus. *Eur. J. Phycol.* 33:281–91.

Hansen, G. & Moestrup, Ø. 1998b. Light and electron microscopical observations on *Peridiniella catenata* (Dinophyceae). *Eur. J. Phycol.* 33:293–305.

Hansen, G., Moestrup, Ø. & Roberts, K. M. 2000. Light and electron microscopical observations on the type species of *Gymnodinium, G. fuscum* (Dinophyceae). *Phycologia* 39:365–76.

Heimann, K., Roberts, K. R. & Wetherbee, R. 1995. Flagellar apparatus transformation and development in *Prorocentrum micans* and *P. minimum* (Dinophyceae). *Phycologia* 34:323–35.

Huber-Pestalozzi, G. 1950. Cryptophyceen, Chloromonadinen, Peridineen. *In* Thienemann, A. [Ed.] *Die Binnengewässer*. Vol. 16. E. Schweizerbart'sche Verlagsbuchhandlung, Stuttgart, 310 pp.

Javornický, P. 1962. Two scarcely known genera of the class Dinophyceae: *Bernardinium* Chodat and *Crypthecodinium* Biecheler. *Preslia* 34:98–113.

Javornický, P. 1997. *Bernardinium* Chodat (Dinophyceae), an athecate dinoflagellate with reverse, right-handed course of the cingulum and transverse flagellum, and *Esoptrodinium* genus novum, its mirror-symmetrical pendant. *Arch. Hydrobiol. Suppl.* 122(Algol. Stud. 87):29–42.

Kawai, H. & Kreimer, G. 2000. Sensory mechanisms. Phototaxes and light perception in algae. *In* Leadbeater, B. S. C. & Green, J. C. [Eds.] *The Flagellates. Unity, Diversity and Evolution*. Taylor & Francis, New York, pp. 124–46 (Systematics Association Special Volume No. 59.) pp. 124–146.

Kremp, A., Elbrächter, M., Schweikert, M., Wolny, J. L. & Gottschling, M. 2005. *Woloszynskia halophila* (Biecheler) comb. nov.: a bloom-forming cold-water dinoflagellate co-occurring with *Scrippsiella hangoei* (Dinophyceae) in the Baltic Sea. *J. Phycol.* 41:629–42.

Leaché, A. D. & Reeder, T. W. 2002. Molecular systematics of the eastern fence lizard (*Sceloporus undulatus*): a comparison of parsimony, likelihood, and Bayesian approaches. *Syst. Biol.* 51:44–68.

Leadbeater, B. S. C. & Dodge, J. D. 1967a. An electron microscope study of nuclear and cell division in a dinoflagellate. *Arch. Mikrobiol.* 57:239–54.

Leadbeater, B. S. C. & Dodge, J. D. 1967b. An electron microscope study of dinoflagellate flagella. *J. Gen. Microbiol.* 46:305–14, pls. 1–4.

Lenaers, G., Maroteaux, L., Michot, B. & Herzog, M. 1989. Dinoflagellates in evolution. A molecular phylogenetic analysis of large subunit ribosomal RNA. *J. Mol. Evol.* 29:40–51.

Lindberg, K., Moestrup, Ø. & Daugbjerg, N. 2005. Studies on woloszynskioid dinoflagellates I: *Woloszynskia coronata* re-examined using light and electron microscopy and partial LSU rDNA sequences, with description of *Tovellia* gen. nov. and *Jadwigia* gen. nov. (Tovelliaceae fam. nov.). *Phycologia* 44: 416–40.

Maddison, D. R. & Maddison, W. P. 2003. *MacClade 4*. Sinauer Associates Inc., Sunderland, MAs, USA.

Matvienko, O. M. & Litvinenko, R. M. 1977. Pirofitovi vodorosti. *In* Hollerbach, M. M. & Kondrat'eva, N. V. [Eds.] *Viznachnyk Prisnovodnykh Vodorostej Ukrains'koj RSR*. Vol. 3(2). Naukova Dumka, Kiev, 386 pp.

Moestrup, Ø. 2000. The flagellate cytoskeleton. Introduction of a general terminology for microtubular flagellar roots in protists. *In* Leadbeater, B. S. C. & Green, J. C. [Eds.] *The Flagellates. Unity, Diversity and Evolution (Systematics Association Special Volume No. 59)*. Taylor & Francis, New York, pp. 69–94.

Moestrup, Ø., Hansen, G., Daugbjerg, N., Flaim, G. & D'Andrea, M. Studies on woloszynskioid dinoflagellates II: on *Tovellia sanguinea* sp. nov., the dinoflagellate species responsible for the reddening of Lake Tovel, N. Italy. *Eur. J. Phycol.* (submitted).

Nichols, H. W. 1973. Growth media—freshwater. *In* Stein, J. R. [Ed.] *Handbook of Phycological Methods. Culture Methods and*

Growth Measurements. Cambridge University Press, Cambridge, pp. 7–24.
Patterson, D. J. 1999. Diversity of eukaryotes. *Am. Nat.* 154: S96–S124.
Pfiester, L. A. 1984. Sexual reproduction. *In* Spector, D. L. [Ed.] *Dinoflagellates*. Academic Press, Orlando, pp. 181–99.
Popovský, J. 1990. New knowledge on freshwater dinoflagellates of Central Europe; with description of a new species. *Arch. Hydrobiol. Suppl.* 87(Algol. Stud. 60):1–18.
Popovský, J. & Pfiester, L. A. 1990. Dinophyceae (Dinoflagellida). *In* Ettl, H., Gerloff, J., Heynig, H. & Mollenhauer, D. [Eds.] *Süßwasserflora von Mitteleuropa*. Vol. 6. Gustav Fischer, Jena, 272 pp.
Posada, D. & Crandall, K. A. 1998. MODELTEST: testing the model of DNA substitution. *Bioinformatics* 14:817–8.
Roberts, K. R., Hansen, G. & Taylor, F. J. R. 1995. General ultrastructure and flagellar apparatus architecture of *Woloszynskia limnetica* (Dinophyceae). *J. Phycol.* 31:948–57.
Roberts, K. R. & Timpano, P. 1989. Comparative analyses of the dinoflagellate flagellar apparatus. I. *Woloszynskia* sp. *J. Phycol.* 25:26–36.
Ronquist, F. & Huelsenbeck, J. P. 2003. Mr. Bayes 3: Bayesian phylogenetic inference under mixed models. *Bioinformatics* 19:1572–4.
Schiller, J. 1935. Dinoflagellatae (Peridineae) in monographischer Behandlung. *In* Kolkwitz, R. [Ed.] *Rabenhorst's Kryptogamenflora von Deutschland, Österreich und der Schweiz*. 2nd ed. Vol. 10, 3 part 2. Akademische Verlagsgesellschaft, Leipzig, pp. 589 [The volume was finished in 1937 but the relevant pages were published in March 1935].
Scholin, C. A., Herzog, M., Sogin, M. & Anderson, D. M. 1994. Identification of group-and strain-specific genetic markers for globally distributed *Alexandrium* (Dinophyceae). II. Sequence analysis of a fragment of the LSU rRNA gene. *J. Phycol.* 30:999–1011.
Spero, H. J. 1982. Phagotrophy in *Gymnodinium fungiforme* (Pyrrhophyta): the peduncle as an organelle of ingestion. *J. Phycol.* 18:356–60.
Spero, H. J. 1985. Chemosensory capabilities in the phagotrophic dinoflagellate *Gymnodinium fungiforme*. *J. Phycol.* 21:181–4.
Starmach, K. 1974. Cryptophyceae, Dinophyceae, Raphidophyceae. *In* Starmach, K. & Sieminska, J. [Eds.] *Flora Słodkowodna Polski*. Vol. 4. Państwowe Wydawnictwo Naukowe, Warszawa, 520 pp.
Stein, F. 1878. *Der Organismus der Infusionsthiere nach eigenen Forschungen in systematischer Reihenfolge bearbeitet. III. Abtheilung. Die Naturgeschichte der Flagellaten oder Geisselinfusorien. I. Hälfte. Den noch nicht Abgeschlossenen allgemeinen Theil nebst Erklärung der sämmtlichen Abbildungen enthaltend*. Wilhelm Engelmann, Leipzig, 154 pp., 24 pls.
Stein, F. 1883. *Der Organismus der Infusionsthiere . . . III. Abtheilung. II. Hälfte. Die Naturgeschichte der arthrodelen Flagellaten. Einleitung und Erklärung der Abbildungen*. Wilhelm Engelmann, Leipzig, 30 pp., 25 pls.
von Stosch, H. A. 1964. Zum Problem der sexuellen Fortpflanzung in der Peridineengattung *Ceratium*. *Helgol. Wiss. Meeresunters.* 10:140–52.
von Stosch, H. A. 1965. Sexualität bei *Ceratium cornutum* (Dinophyta). *Naturwissenschaften* 52:112–3.
von Stosch, H. A. 1973. Observations on vegetative reproduction and sexual life cycles of two freshwater dinoflagellates, *Gymnodinium pseudopalustre* Schiller and *Woloszynskia apiculata* sp. nov. *Br. Phycol. J.* 8:105–34.
Swofford, D. L. 2003. *PAUP* Phylogenetic Analysis Using Parsimony (*and Other Methods). Version 4*. Sinauer Associates, Sunderland, MA.
Tamura, K. & Nei, N. 1993. Estimation of the number of nucleotide substitutions in the control region of mitochondrial DNA in humans and chimpanzees. *Mol. Biol. Evol.* 10:512–26.
Thompson, R. H. 1951. A new genus and new records of freshwater Pyrrophyta in the Desmokontae and Dinophyceae. *Lloydia* 13:277–99.
Van de Peer, Y., Van der Auwera, G. & de Wachter, R. 1996. The evolution of stramenopiles and alveolates as derived by "substitution rate calibration" of small ribosomal RNA. *J. Mol. Evol.* 42:201–10.
Wawrik, F. 1983. Sommerliche Planktonaspekte 1981: seltene und neue Algen aus Teichen des Waldviertels in Niederösterreich. *Nova Hedwigia* 36:775–94.
Wedemayer, G. J. & Wilcox, L. W. 1984. The ultrastructure of the freshwater colorless dinoflagellate *Peridiniopsis berolinense* (Lemm.) Bourrelly. *J. Protozool.* 31:444–53.
Wilcox, L. W. 1989. Multilayered structures (MLSs) in two dinoflagellates, *Katodinium campylops* and *Woloszynskia pascheri*. *J. Phycol.* 25:785–9.
Wołoszyńska, J. 1917. Nowe gatunki Peridineów, tudziez spostrzezenia nad budowa okrywy u Gymnodiniów i Glenodiniów.—Neue Peridineen-Arten, nebst Bemerkungen über den Bau der Hülle bei *Gymno-* und *Glenodinium*. *Bull. Int. Acad. Sci. Cracovie, Cl. Sci. Math. Nat., Ser. B* 1917:114–22, pls. 11–13.
Yang, Z. & Rannala, B. 1997. Bayesian phylogenetic inference using DNA sequences: a Markov chain Monte Carlo method. *Mol. Biol. Evol.* 14:717–24.